UNIVERSITY OF CALIFORNIA SAN DIEGO

Drug screening and discovery against the human intestinal parasite *Entamoeba histolytica*

A dissertation submitted in partial satisfaction of the
requirements for the degree
Doctor of Philosophy

in

Biomedical Sciences

by

Conall Sauvey

Committee in charge:

Professor Ruben Abagyan, Chair
Professor James McKerrow, Co-Chair
Professor Carlo Ballatore
Professor Lars Eckmann
Professor Sanjay Nigam

2021

The Dissertation of Conall Sauvey is approved, and it is acceptable in quality and form for publication on microfilm and electronically.

University of California San Diego

2021

DEDICATION

To my mother, Dr. Mary Sauvey, for her many years of love and support, and for giving me the curiosity and love of learning that led me to become a scientist.

And to my wife Yashna, for her love, encouragement, and belief in me. With her around, even the hardest parts of completing a doctoral dissertation can be joyful.

TABLE OF CONTENTS

Dissertation approval page iii
Dedication iv
Table of contents v
List of figures vi
List of tables vii
List of abbreviations viii
List of supplementary files ix
Acknowledgements x
Vita xi
Abstract of the Dissertation xii
Chapter 1 Antineoplastic kinase inhibitors: a new class of potent anti-amoebic compounds 1
Chapter 2 High-throughput phenotypic screen identifies a new family of potent anti-amoebic compounds 45

LIST OF FIGURES

Figure 1.1 EC_{50} determination of antineoplastic kinase inhibitors against *E. histolytica* trophozoites. 8

Figure 1.2 Generation of human target profile for inhibitors of *E. histolytica.* 10

Figure 1.3 Graphical screening workflow of antineoplastic kinase inhibitors against *E. histolytica.* 11

Figure 1.4 In silico screen based on human target profile to determine new potent amoebicidal drug candidates. 12

Figure 1.5 Network map of active drug profile proteins with orthologous *E. histolytica* ORFs. 15

Figure 1.6 Extended screen of antineoplastic kinase inhibitors against *E. histolytica* trophozoites. 18

Figure 1.7 Amoebicidal effects of antineoplastic kinase inhibitor drugs. 20

Figure 1.8 Timing of drug action against *E. histolytica* trophozoites. 22

Figure 1.9 Activity of antineoplastic kinase inhibitors against *Entamoeba* cysts. 25

Supplementary figure 1.10 False-positive assay against *E. histolytica* trophozoites. 43

Figure 2.1. High-throughput screening results of 81,664 small molecules against *E. histolytica*. 50

Figure 2.2. EC_{50} determination assay identifies a highly potent inhibitor of *E. histolytica*. 52

Figure 2.3. Cell counting assay confirms anti-amoebic activity of compound JNJ001. 55

Figure 2.4. Compound JNJ001 does not inhibit human HEK293 cells. 57

Figure 2.5. Compound JNJ001 achieves peak anti-amoebic effects within 24-36 hours. 59

Figure 2.6. Compound JNJ001 inhibits *E. invadens* cysts. 61

Figure 2.7. Dose-response assay results for Jump-stARter library JNJ001 series expansion compounds. 65

Figure 2.8. Structures of Jump-stARter library JNJ001 series expansion compounds. 66

Figure 2.9. Dose-response assay results for non-Jump-stARter library JNJ001 series expansion compounds. 67

Figure 2.10. Structures of non-Jump-stARter library JNJ001 series expansion compounds. 68

Figure 2.11. Series expansion compounds do not cause cell death in human HEK293 cells. 70

LIST OF TABLES

Table 1.1 Results of primary screen of AKI drugs against *E. histolytica* trophozoites. 7

Table 1.2 Analysis of drugs based on activity towards individual proteins in the active drug target profile. 13

Table 1.3 Results of extended screen of AKI drugs against *E. histolytica* trophozoites. 17

Table 1.4 A selection of published data regarding the adverse effects of 1-2 doses of AKI drugs of interest in healthy subjects. 29

Table 1.5 Published pharmacokinetic data for AKI drugs of interest following 1-2 doses in healthy subjects. 31

Table 2.1 EC_{50} values of top hits from high-throughput screen. 53

Table 2.2 EC_{50} values of Jump-stARter library JNJ001 series expansion compounds against *E. histolytica* trophozoites in vitro. 63

Table 2.3 EC_{50} values of non-Jump-stARter library JNJ001 series expansion compounds against *E. histolytica* trophozoites in vitro. 64

LIST OF ABBREVIATIONS

EC_{50}: Half maximal effective concentration of a drug or chemical agent

AKI: Antineoplastic kinase inhibitor

CDM: Cancer drug map software tool

ORF: Open reading frame

pAct: -log(a measure of drug or chemical agent activity)

T_{max}: Measured time until maximal blood plasma concentration of a drug or chemical agent is reached

C_{max}: Maximal measured blood plasma concentration of a drug or chemical agent

$T_{1/2}$: Half-life of a drug or chemical agent

SAR: Structure-activity relationship

LIST OF SUPPLEMENTARY FILES

Chapter 1 data files:

Supplementary dataset 1.1 Figure 1.1 Data. (XLSX)

Supplementary dataset 1.2 Figure 1.6 Data. (XLSX)

Supplementary dataset 1.3 Figure 1.7 Data. (XLSX)

Supplementary dataset 1.4 Figure 1.8 Data. (XLSX)

Supplementary dataset 1.5 Figure 1.9 Data. (XLSX)

Supplementary dataset 1.6 Figure 1.S1 Data. (XLSX)

Chapter 2 data files:

Supplementary dataset 2.1 Figure 1 data. (XLSX)

Supplementary dataset 2.2 384-well dose-response screen data. (XLSX)

Supplementary dataset 2.3 Figure 2 data. (XLSX)

Supplementary dataset 2.4 Figure 3 data. (XLSX)

Supplementary dataset 2.5 Figure 4 data. (XLSX)

Supplementary dataset 2.6 Figure 5 data. (XLSX)

Supplementary dataset 2.7 Figure 6 data. (XLSX)

Supplementary dataset 2.8 Figure 7 data. (XLSX)

Supplementary dataset 2.9 Figure 9 data. (XLSX)

Supplementary dataset 2.10 Figure 11 data. (XLSX)

ACKNOWLEDGEMENTS

I would like to acknowledge Professor Ruben Abagyan for his mentorship throughout my doctoral studies, for always working to help me find the best opportunities and achieve my potential, and for guiding me on the path to becoming a true scientist.

I would like to acknowledge Dr. Jonathan Blevitt and Professor Anjan Debnath for their crucial guidance in technical, practical, and strategic aspects of my research efforts.

I would like to thank Professor James McKerrow for generously providing access to many of the key resources and equipment that were indispensable to my research.

I would also like to thank several past and present members of the Abagyan, Singh, McKerrow, and other labs for their invaluable assistance with many aspects of my graduate studies. In particular I would like to thank (in rough chronological order): Lily Hahn, Thi Nguyen, Abdolhakim Mohammed, Jair Lage Siqueira Neto, Ken Hirata, Ittipat Meewan, Jean Bernatchez, Danielle Skinner, Armin Faroughi, Kirti Khandwal Chahal, and Monica Mendes Kangussu Marcolino – without them this research would not have been possible.

Chapter 1, in part, is a reprint of the material as it may appear in PLOS Neglected Tropical Diseases, 2021, Conall Sauvey, Gretchen Ehrenkaufer, Da Shi, Anjan Debnath, Ruben Abagyan. The dissertation author was the primary investigator and author of this paper.

Chapter 2, in part, has been submitted for publication of the material as it may appear in PLOS Neglected Tropical Diseases, 2021, Conall Sauvey, Gretchen Ehrenkaufer, Jonathan Blevitt, Paul Jackson, Ruben Abagyan. The dissertation author was the primary investigator and author of this paper.

VITA

2009-2013 Bachelor of Science, Genetics, University of Wisconsin - Madison

2014-2021 Doctor of Philosophy, Biomedical Sciences, University of California San Diego

PUBLICATIONS

First Author

Antineoplastic kinase inhibitors: A new class of potent anti-amoebic compounds. *PLOS Neglected Tropical Diseases*. 2021

High-throughput phenotypic screen identifies a new family of potent anti-amoebic compounds. *Submitted: PLOS Neglected Tropical Diseases*. 2021

Other Authorship

ARN25068, a versatile starting point for neurodegenerative disorders: paving the way to triple GSK-3β/FYN/DYRK1A inhibitors to tackle aberrant tau phosphorylation. *In Review: Journal of Medicinal Chemistry. 2021*

A simple and efficient system for regulating gene expression in human pluripotent stem cells and derivatives. *Stem Cells.* 2014

Directed differentiation of forebrain GABA interneurons from human pluripotent stem cells. *Nature Protocols*. 2013

ABSTRACT OF THE DISSERTATION

Drug screening and discovery against the human intestinal parasite *Entamoeba histolytica*

by

Conall Sauvey

Doctor of Philosophy in Biomedical Sciences

University of California San Diego, 2021

Professor Ruben Abagyan, Chair

Professor James McKerrow, Co-Chair

Entamoeba histolytica is a protozoan amoeba and human parasite which causes the disease amoebiasis, also known as amoebic colitis. The World Health Organization estimates that at any given time approximately 50 million people worldwide are hosts to *E. histolytica* parasites, resulting in an

estimated 50,000 to 70,000 deaths each year. Unfortunately, due to the fecal-oral transmission route of *E. histolytica*, it most severely affects socieoeconomically vulnerable populations experiencing difficulty in accessing clean water and food. For many years this disease has been treated using the nitroimidazole drug metronidazole. However, notable drawbacks to this drug do exist, such as strong adverse effects and the need for followup treatments in order to eliminate the transmissible cyst stage of *E. histolytica*. Due to these and other factors, the search for new and different drugs that kill *E. histolytica* remains urgent and ongoing.

Here I present two studies in which my co-authors and I contributed to this search using two different screening approaches, allowing us to identify multiple highly potent anti-amoebic compounds with various favorable properties for further development as potential treatments for amoebiasis.
In the first study, we conducted a small, targeted screen of FDA-approved kinase inhibitor drugs for their ability to kill *E. histolytica* trophozoites in vitro and identified potent activity among a number of candidates. Using computational analyses, we were then able to further refine the results of this initial screen and identify additional drugs with even higher potency, as well as additional desirable properties such as inhibition of infective Entamoeba cysts.

In the second study, we collaborated with Janssen pharmaceuticals to obtain an 80,000-member chemical library, and used it to conduct a high-throughput screen for inhibitors of *E. histolytica* growth and survival. From this screen we identified a new highly-potent inhibitor molecule, as well as several additional, structurally-related inhibitors. Further experimentation showed this compound to possess desirable properties such as inhibition of Entamoeba cysts, and non-toxicity to cultured human cells. Together these studies document the discovery of two novel families of highly-effective anti-amoebic drugs with strong potential for further development as treatments against this devastating disease

CHAPTER 1 ANTINEOPLASTIC KINASE INHIBITORS: A NEW CLASS OF POTENT ANTI-AMOEBIC COMPOUNDS

Abstract

Entamoeba histolytica is a protozoan parasite which infects approximately 50 million people worldwide, resulting in an estimated 70,000 deaths every year. Since the 1960s *E. histolytica* infection has been successfully treated with metronidazole. However, drawbacks to metronidazole therapy exist, including adverse effects, a long treatment course, and the need for an additional drug to prevent cyst-mediated transmission. *E. histolytica* possesses a kinome with approximately 300 - 400 members, some of which have been previously studied as potential targets for the development of amoebicidal drug candidates. However, while these efforts have uncovered novel potent inhibitors of *E. histolytica* kinases, none have resulted in approved drugs. In this study we took the alternative approach of testing a set of twelve previously FDA-approved antineoplastic kinase inhibitors against *E. histolytica* trophozoites *in vitro*. This resulted in the identification of dasatinib, bosutinib, and ibrutinib as amoebicidal agents at low-micromolar concentrations. Next, we utilized a recently developed computational tool to identify twelve additional drugs with human protein target profiles similar to the three initial hits. Testing of these additional twelve drugs led to the identification of ponatinib, neratinib, and olmutinib were identified as highly potent, with EC_{50} values in the sub-micromolar range. All of these six drugs were found to kill *E. histolytica* trophozoites as rapidly as metronidazole. Furthermore, ibrutinib was found to kill the transmissible cyst stage of the model organism *E. invadens*. Ibrutinib thus possesses both amoebicidal and cysticidal properties, in contrast to all drugs used in the current therapeutic strategy. These findings

together reveal antineoplastic kinase inhibitors as a highly promising class of potent drugs against this widespread and devastating disease.

Introduction

Entamoeba histolytica is a parasitic amoeba which infects an estimated 50 million people worldwide, resulting in around 70,000 deaths per year [1]. *E. histolytica* infection is known as amoebiasis and primarily affects the intestinal tract in humans, most commonly causing symptoms such as abdominal pain, bloody diarrhea, and colitis [2]. In rare cases the infection spreads to other organs such as the liver and brain, and in serious cases results in patient death [2]. *E. histolytica*'s life cycle consists of a trophozoite vegetative stage which matures in its host to an infective cyst stage. The cyst stage is excreted in the host's feces, infecting a new host when ingested via a route such as drinking contaminated water. In the majority of cases where *E. histolytica* is ingested it lives asymptomatically in the human host's intestinal tract. Symptoms can develop when compromise of the mucosal layer allows it to come into contact with the intestinal wall, at which point it invades the wall and surrounding tissue causing characteristic 'flask-shaped ulcers' [3]. Due to this mode of transmission *E. histolytica* disproportionately affects populations experiencing sanitation problems associated with low socioeconomic status [2, 4, 5]. Malnutrition is also known to be a major risk factor for amoebiasis, especially in children [6].

E. histolytica infection is currently treated with the 5-nitroimidazole drug metronidazole, which has been in use since the 1960s and has widespread use as a treatment against anaerobic microbial infection [7, 8]. However, while successful, metronidazole is not a perfect solution to *E. histolytica* infection, with a few particularly notable existing issues. One of these is problems with lack of patient compliance with the full course of treatment, leading to relapses and increased disease spread [7]. This is possibly due to factors such as drug adverse effects or the need for continued dosing past the resolution of disease symptoms [9, 10]. Another issue is metronidazole's inability to kill the infective cyst stage of *E. histolytica*. Because of this, along with its complete absorbance from the intestines, metronidazole must

be followed by a secondary luminal amoebicide such as paromomycin to prevent spread of the disease [11, 12]. Also concerning is the potential for the emergence of resistance to metronidazole, which has been previously observed in the laboratory [13]. When considered together, these factors comprise an unmet need for alternative amoebiasis therapies.

Several efforts to find such alternative therapies have been undertaken over the years, including the recent development of the antirheumatic drug auranofin as a promising potential treatment for amoebiasis [14-16]. One noteworthy direction of anti-amoebic drug research has been the efforts of multiple groups to inhibit *E. histolytica* by targeting specific kinase proteins believed to be critical to the parasite's functioning [17-19]. This approach has often involved computational modeling and *in-silico* screening of compounds against the kinases of interest, followed by *in-vitro* tests of top-scoring molecules [17]. These efforts have resulted in both the discovery of potent new hit compounds as well as validation of the previously discovered activity of auranofin [17]. Auranofin passed a new Phase 1 trial and was poised to be evaluated in a clinical trial in Bangladesh until that trial was halted due to the Covid-19 pandemic [20]. Therefore there are no new clinically sanctioned treatments for amebiasis.

Importantly, one promising area currently unexplored by such studies is the potential of existing human kinase inhibitor drugs. A particular advantage of these drugs is the rich array of data available regarding their activity profiles against human target proteins, which allows for the mapping and utilization of their complex multi-target pharmacology. Such maps could in turn be projected into the *E. histolytica* proteome and used to infer potential antiamoebic drug activity by identifying drugs with similar target profiles to known active compounds. We have previously published a computational tool capable of such mapping for antineoplastic drugs, including a large number of kinase inhibitors [20]. We describe here the use of this tool to prioritize molecules for screening against *E. histolytica* trophozoites based on initial hits from a small primary screen. In total, 6 antineoplastic kinase inhibitors (AKIs) were

found to have potent and rapid anti-amoebic activity. The results of these experiments demonstrate the promise of using target-based analysis to leverage compounds with multi-target pharmacology against a human parasite.

Results

Screen of antineoplastic kinase inhibitors against *E. histolytica* trophozoites

In order to identify anti-amoebic activity among antineoplastic kinase inhibitors, a selection of 12 drugs was screened against *E. histolytica* trophozoites *in vitro*. All compounds tested were FDA-approved cancer chemotherapy drugs designed to inhibit human kinase proteins as their mechanism of action. *E. histolytica* trophozoites were seeded into 96-well plates along with a serially-diluted range of drug concentrations. Trophozoites were incubated for 48 hours, after which the surviving cell count was determined using a luciferase-based cell viability assay. Percent inhibition of trophozoite growth was calculated for each treatment well in comparison with vehicle-only negative controls representing 0% inhibition, and media-only or metronidazole-treated positive controls representing 100% inhibition. From this data EC_{50} values were calculated for each respective drug (Table 1). Of the 12 drugs tested, ibrutinib, dasatinib, and bosutinib all were found to possess EC_{50} values similar to or lower than the EC_{50} values of of 2-5 μM for the currently used drug metronidazole (Fig 1). Based on these results we concluded that antineoplastic kinase inhibitor drugs are capable of potent inhibition of *E. histolytica* and determined that further analysis and refinement was warranted in order to discover even more potent drugs in the same class.

Table 1.1 Results of primary screen of AKI drugs against *E. histolytica* trophozoites.

Drug name	EC_{50} (µM)	Anti-amoebic activity
Ibrutinib	0.98	Very high
Dasatinib	1.57	High
Bosutinib	1.94	High
Nilotinib	8.22	Moderate
Gefitinib	8.52	Moderate
Sunitinib	10.09	Low
Afatinib	11.69	Low
Crizotinib	12.83	Low
Erlotinib	42.07	Very low
Dabrafenib	55.18	Very low
Vemurafenib	>100	None
Imatinib	>100	None

Color scale indicates drug potency: darker blue = more potent, lighter blue = less potent. Anti-amoebic activity classified based on EC_{50} value as: Very high (0.001 - 0.999 µM), High (1.000 - 4.999 µM), Moderate (5.000 - 9.999 µM), Low (10.000 - 19.999 µM), Very low (20.000 - 99.999 µM), or None (EC_{50} > 100.000 µM).

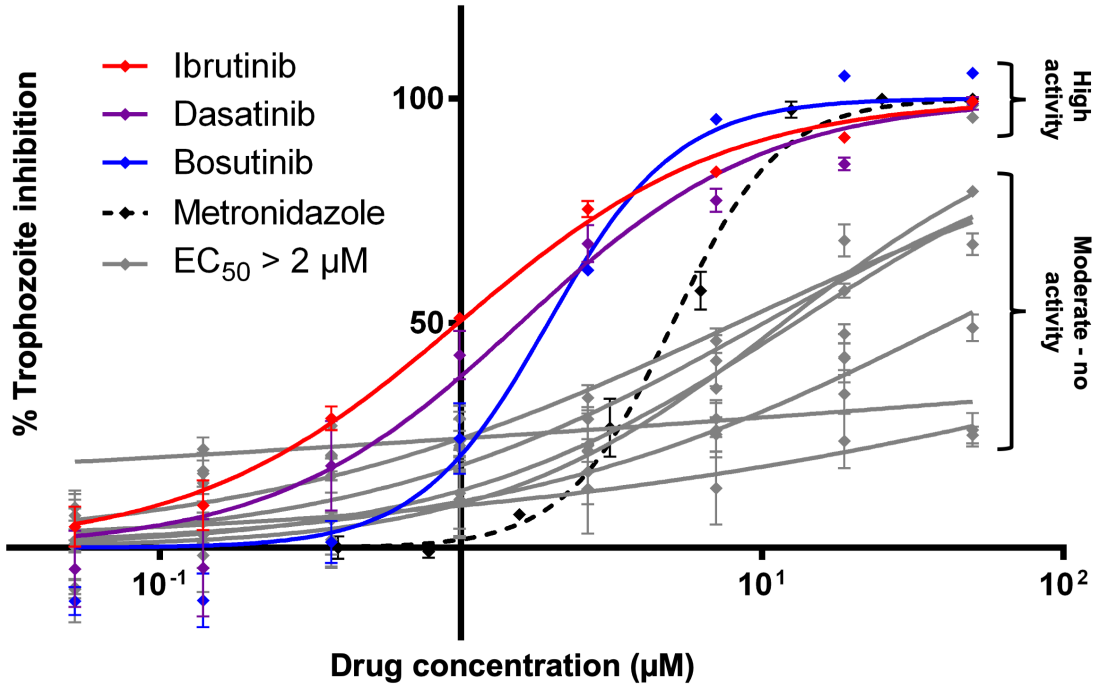

Figure 1.1 EC_{50} determination of antineoplastic kinase inhibitors against *E. histolytica* trophozoites. Dose response curve plotting percentage inhibition of *E. histolytica* trophozoites compared to drug concentrations of antineoplastic kinase inhibitors. The three drugs with the lowest EC_{50} values (ibrutinib, dasatinib, and bosutinib) are plotted in red, purple, and blue. All drugs with EC_{50} values > 2 µM are plotted in gray. Each data point represents mean values of percentage inhibition. Error bars represent standard deviation. Complete list of drugs can be found in Table 1.

Analysis of hits

In order to identify potent anti-amoebic candidates from the existing pool of AKI drugs, an approach was utilized wherein human protein target profiles were computationally generated for drugs active in the screen, followed by identification of additional drugs with matching or similar target profiles. To generate the target profiles for active drugs, a computational tool called CancerDrugMap (CDM) . This tool has been previously described, and is available at: *ruben.ucsd.edu/dnet/* [20]. Using CDM, human targets of both the active and inactive compounds from the initial were compared. Protein targets were scored and ranked based on targeting activity of active compounds as well as lack of targeting activity by the inactive ones. This generated a profile of human protein targets associated with the active amoebicidal drugs in the screen (Fig 2). Based on this profile, two strategies were then employed to identify drugs with similar target profiles and hence the potential for similar anti-amoebic activity (Fig 3). In the first strategy, CDM was used to score and rank all AKI drugs in the database based on their activity against the complete ranked target profile, using an algorithm described in the methods. Drugs possessing a score greater than or equal to 15 were selected for further *in vitro* testing (Fig 4). The second strategy was identical to the first with the exception that CDM was used to score and rank drugs based on activity against target proteins individually rather than the complete profile. Drugs active above a threshold score of 15 against individual proteins from the target profile were ranked by the number of proteins from the profile they possessed this level of activity against (Table 2). Drugs possessing a score at or over the threshold of 15 against more than 2 proteins from the target profile were selected for further investigation. The first and second strategies combined generated a list of 15 drugs with similar known human protein targets to the positive hits from the initial screen, and hence high potential for corresponding anti-amoebic activity.

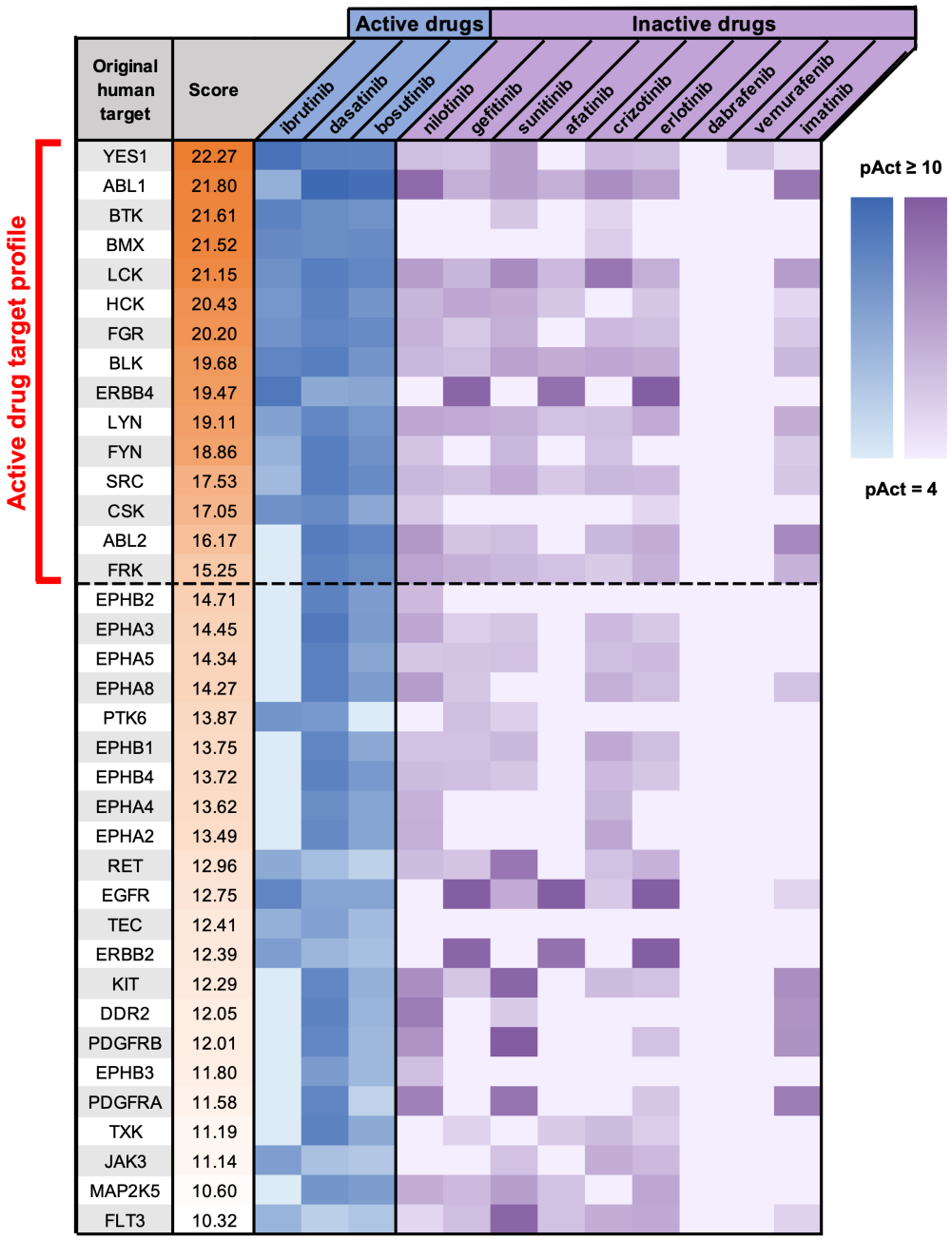

Figure 1.2 Generation of human target profile for inhibitors of *E. histolytica.*
Human kinase proteins scored and ranked based on targeting activity data for active drugs versus inactive drugs from the screen. Heatmap represents the calculated activity values (pAct, see Methods) of individual drugs against individual human protein targets. Darker colors indicate stronger drug activity against the protein. Dashed line represents the cutoff pAct value for proteins to be included in the target profile for the purpose of identifying additional *E. histolytica* drug candidates.

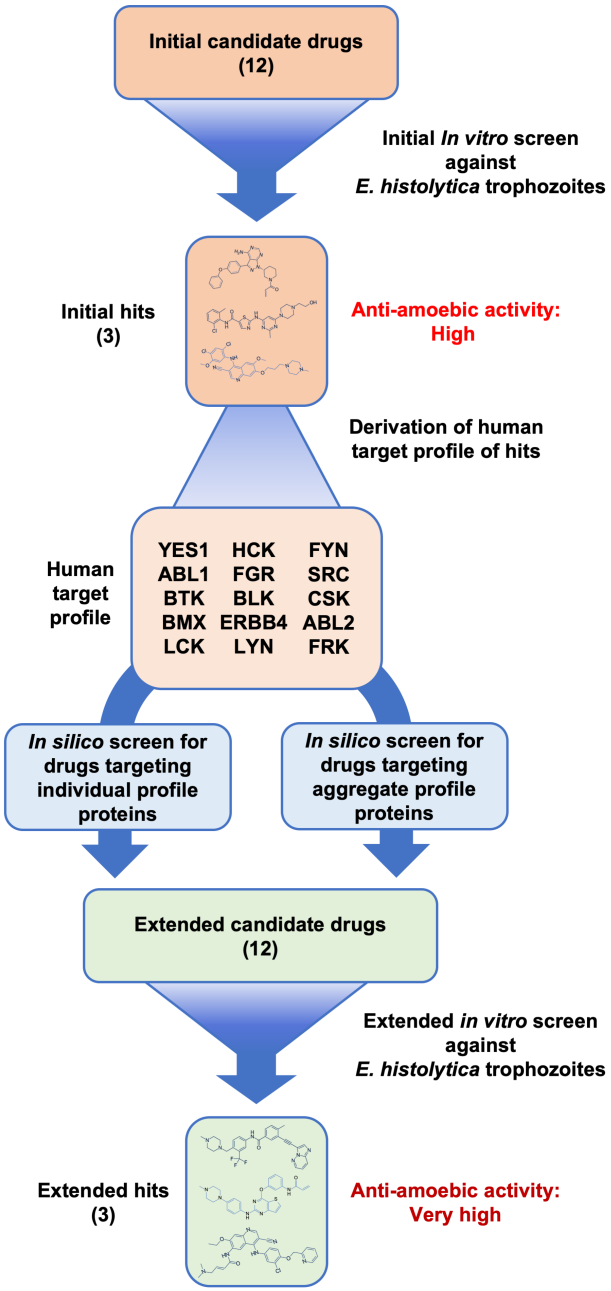

Figure 1.3 Graphical screening workflow of antineoplastic kinase inhibitors against *E. histolytica.* Chemical structures represent the three drugs found to possess the lowest EC_{50} values in each screen (ibrutinib, dasatinib, bosutinib, and ponatinib, neratinib, olmutinib respectively).

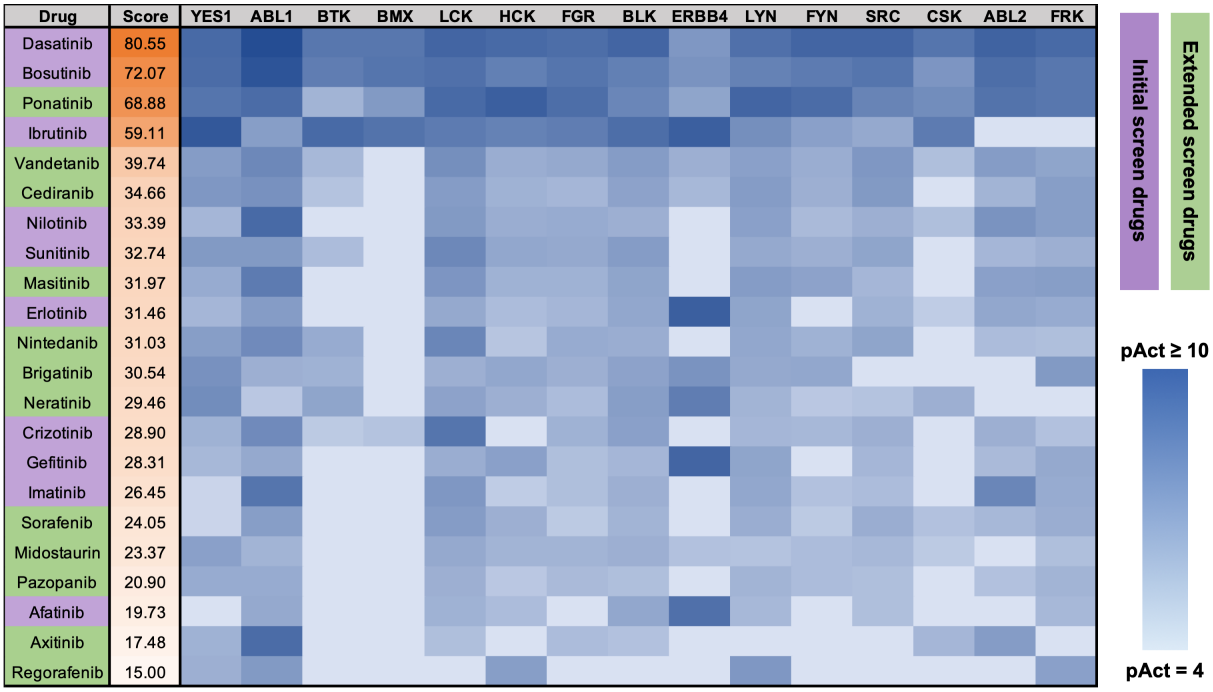

Figure 1.4 In silico screen based on human target profile to determine new potent amoebicidal drug candidates.

Antineoplastic kinase inhibitor drugs scored and ranked based on activity data regarding all 15 proteins in the amoebicidal drug target profile shown in figure 3. Score shown in the second column is calculated from the weighted sum of pAct values (see methods.) Shown are all drugs meeting the cutoff score of 15 for further screening. Heatmap displays the calculated pAct of individual drugs against individual protein targets. Darker colors indicate stronger drug activity against the protein. Purple highlight indicates drugs included in the initial *in vitro* screen. Green highlight indicates new candidate drugs.

Table 1.2 Analysis of drugs based on activity towards individual proteins in the active drug target profile.

Drug name	Number of target profile matches
Dasatinib	15
Bosutinib	15
Ponatinib	13
Ibrutinib	11
Vandetanib	6
Cediranib	6
Sunitinib	4
Nilotinib	4
Masitinib	4
Regorafenib	3
Nintedanib	3
Neratinib	3
Imatinib	3
Brigatinib	3
Acalabrutinib	3
Sorafenib	2
Olmutinib	2
Erlotinib	2
Crizotinib	2
Axitinib	2
Rociletinib	1
Osimertinib	1
Lapatinib	1
Gefitinib	1
Afatinib	1

Drugs are ranked based on the number of proteins from the active drug target profile towards which they possess an activity score greater than a threshold value. Darker color indicates a greater number of proteins. Drugs possessing the desired level of activity towards more than two target profile proteins were considered for further screening, shown above red line.

Potential drug target proteins are present in the *E. histolytica* proteome

While the data regarding activity of AKI drugs against human target proteins is valuable for the purpose of grouping drugs with the potential for similar activity against *E. histolytica*, it does not provide information regarding the drugs' actual protein targets in the parasite. In order to identify whether potential drug targets exist in *E. histolytica* that are similar to the human target profile proteins, the human proteins were searched against the *E. histolytica* proteome. In order to do so, the kinase domain sequences of the human proteins were extracted and aligned against the complete published set of *E. histolytica* open reading frames (ORFs). 32 *E. histolytica* ORFs were found to align to the human sequences with a p-value of 10^{-10} or less. A network map was generated of these top-scoring *E. histolytica* proteins and their relationship to the human protein targets (Fig 5). In the network map multiple *E. histolytica* ORFs can be seen to possess strong alignments to several human sequences. These results demonstrate the possibility that *E. histolytica* may possess protein targets equivalent to those known to be targeted in humans by the active AKI drugs.

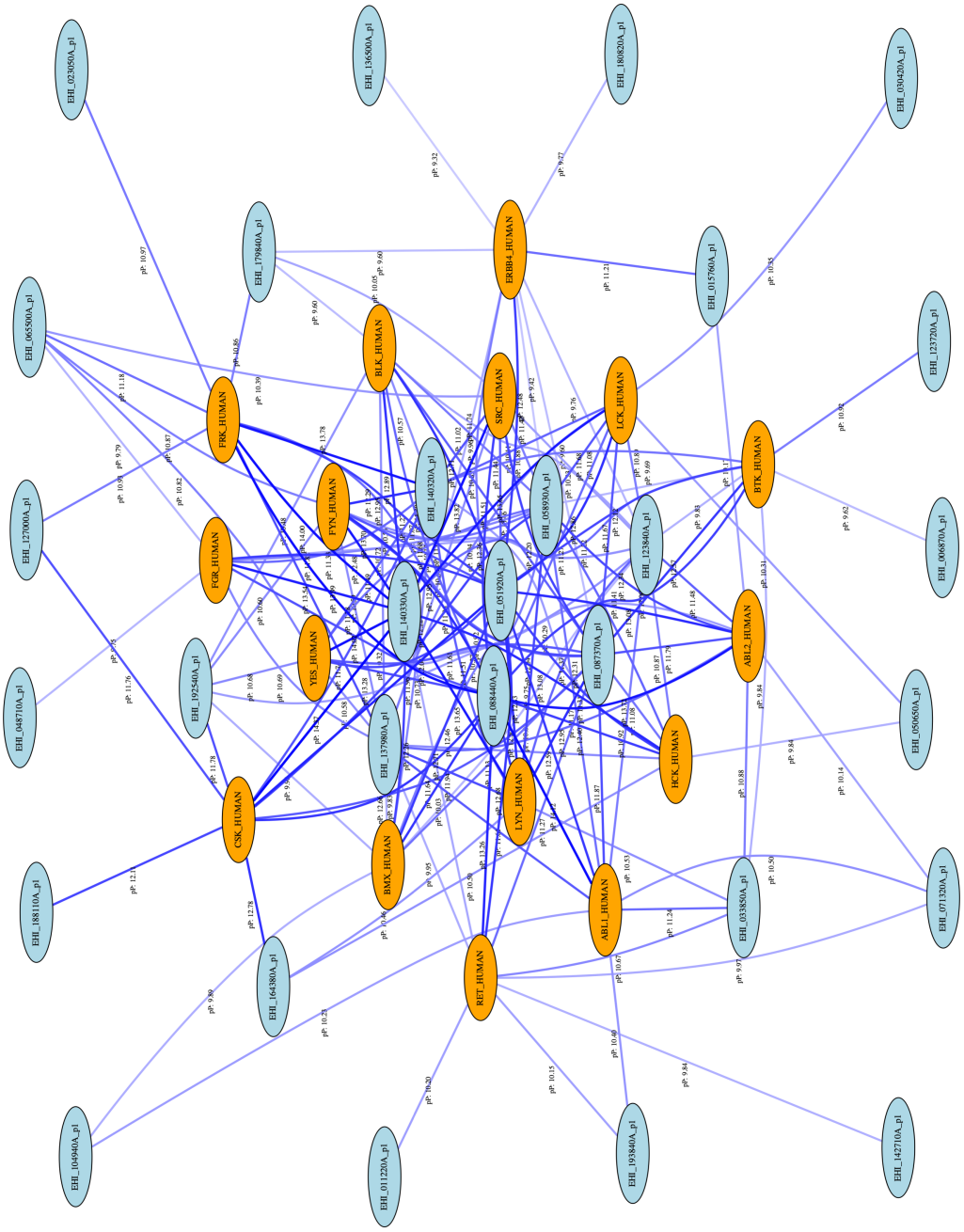

Figure 1.5 Network map of active drug profile proteins with orthologous *E. histolytica* ORFs. Orange ovals represent human sequences. Blue ovals represent *E. histolytica* sequences. Lines represent alignment relationships possessing a calculated pP greater than the cutoff value of 10. Line color represents pP value, with darker lines denoting higher pP. Blue ovals shown in the center with the highest number of connecting lines represent the most likely *E. histolytica* orthologs of the human target proteins.

Extended screen of candidate drugs based on primary analysis

Based on our CDM analysis we tested the list of 12 potentially active AKI drugs against *E. histolytica* trophozoites in an extended *in vitro* screen. Compounds were tested as previously, using the same luciferase-based cell viability assay to determine EC_{50} values. The drugs ponatinib, neratinib, and olmutinib were found to possess highly potent activity in this screen, all with sub-micromolar EC_{50} values (Table 3) (Fig 6).

Table 1.3 Results of extended screen of AKI drugs against *E. histolytica* trophozoites.

Drug name	EC_{50} (µM)	Anti-amoebic activity
Ponatinib	0.1299	Very high
Neratinib	0.3113	Very high
Olmutinib	0.6462	Very high
Nintedanib	4.239	High
Cediranib	7.286	Moderate
Vandetanib	8.971	Moderate
Acalabrutinib	11.34	Low
Masitinib	14.03	Low
Regorafenib	15.94	Low
Sorafenib	18.3	Low
Pazopanib	>100	None
Axitinib	>100	None

Color scale indicates drug potency: darker blue = more potent, lighter blue = less potent. Anti amoebic activity classified based on EC_{50} value as: Very high (0.001 - 0.999 µM), High (1.000 - 4.999 µM), Moderate (5.000 - 9.999 µM), Low (10.000 - 19.999 µM), Very low (20.000 - 99.999 µM), or None (EC_{50} > 100.000 µM).

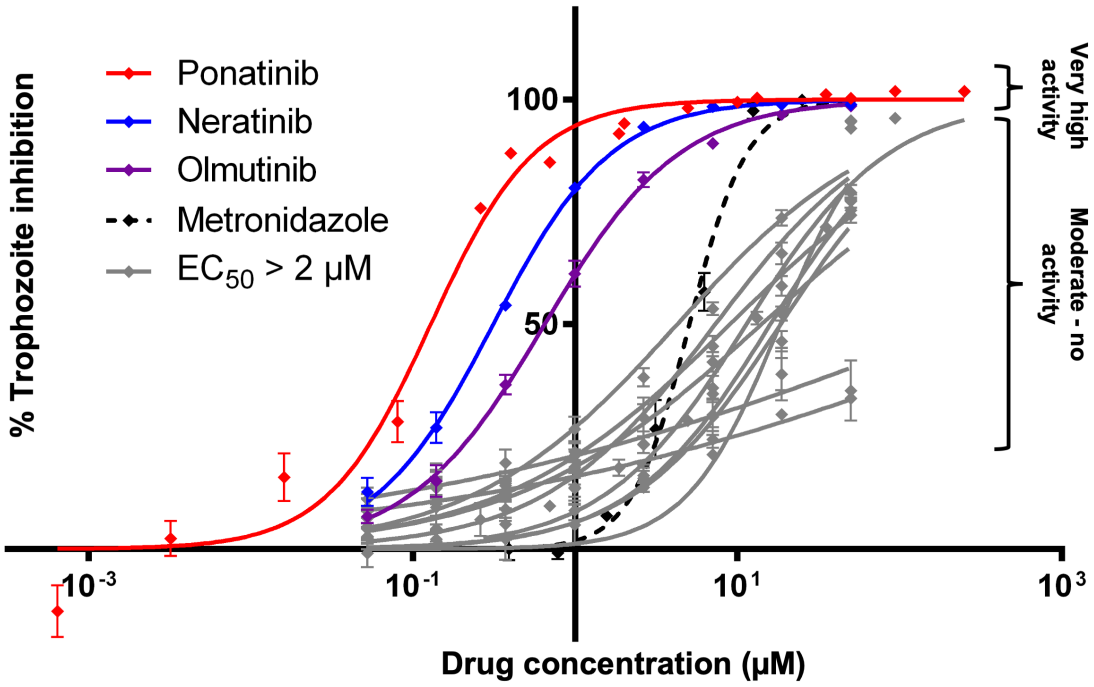

Figure 1.6 Extended screen of antineoplastic kinase inhibitors against *E. histolytica* trophozoites. Dose response curves plotting percentage inhibition of *E. histolytica* trophozoites at different drug concentrations. The three drugs with the lowest EC_{50} values (ponatinib, neratinib, and olmutinib) are plotted in red, purple, and blue. All drugs with EC_{50} values > 2 µM are plotted in gray. Each data point represents mean values. Error bars represent standard deviation. Complete list of drugs tested found in Table 3.

Hit compounds kill *E. histolytica* trophozoites

An important question regarding the activity of any compound intended to act against *E. histolytica* is whether it induces cell death in the parasite or merely slows its replication. In order to determine which type of activity belongs to each of the AKI drugs active in the initial and extended screens, we measured the number of surviving cells after 48 hours of drug treatment compared to freshly-counted aliquots of cells. 5,000 cells per well were seeded into 96-well plates and treated with 10μM of dasatinib, bosutinib, ibrutinib, ponatinib, neratinib, olmutinib, metronidazole, or vehicle. After 48 hours fresh aliquots containing a known number of cells were seeded into empty wells, CellTiter-Glo was added, and the luminescence of all wells was measured. Using the linear relationship of CellTiter-Glo luminescence to the number of cells being assayed, the number of cells in treatment group wells was calculated using their luminescence values relative to those of the freshly-aliquoted wells. All drugs tested were found to have significantly decreased the number of live cells in their treatment groups below the initial 5,000 cells. In contrast, cells treated with only vehicle significantly increased in number to over 14,000 cells per well (Fig 7).

In order to characterize whether the active drugs genuinely kill *E. histolytica* trophozoites or merely act as false positives by inhibiting the ATP-driven, luciferase-based CellTiter-Glo assay system we tested concentration ranges of each drug on cells and immediately after addition of drugs. If the drugs were acting on the CellTiter-Glo assay reagents rather than the cells themselves, a dose-response relationship of drug to assay activity should have been evident. However, no dose-response relationship was observed, and measured luminescence values remained equivalent across all concentrations of drug treatments. (S1 Fig) These results indicate that the active drugs are true positives against *E. histolytica* cells and do not inhibit the assay itself.

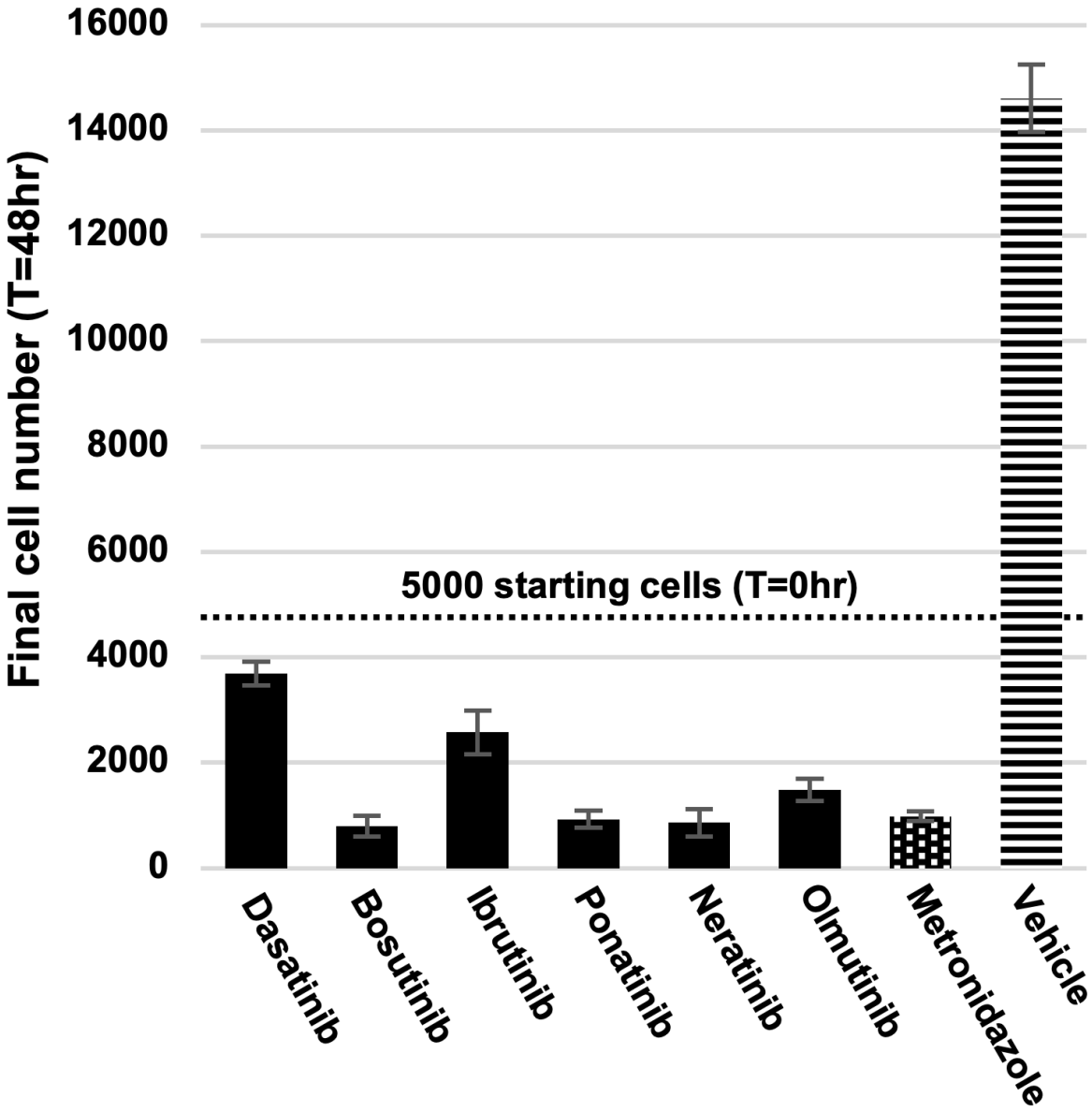

Figure 1.7 Amoebicidal effects of antineoplastic kinase inhibitor drugs.
Live cell number calculated in comparison to aliquots of known amounts of cells. All drugs tested at 10μM, vehicle = 0.5% DMSO. Dotted line represents the 5000 cells originally seeded into all wells for each treatment group. Error bars represent standard deviation.

Hit compounds kill *E. histolytica* trophozoites as rapidly as metronidazole

In addition to drug potency, an important characteristic of any drug is the rapidity with which it achieves its desired effect. In order to characterize this aspect of the most active drugs from the trophozoite viability screens, the EC_{50} values of ponatinib, neratinib, olmutinib, and metronidazole against *E. histolytica* trophozoites were measured at a series of timepoints after treatment initiation. The luciferase-based CellTiter-Glo cell viability assay was used as previously to determine the percent inhibition in each set of experimental replicates. Duplicate plates containing cells treated with serially-diluted ranges of ponatinib, neratinib, olmutinib, and metronidazole concentrations were prepared for each desired time point. Measurements were collected at 12, 24, 36, and 48 hours post-drug-treatment respectively. From the data obtained EC_{50} values were calculated for each time point of each drug treatment and compared over time (Fig 8A-D). All drugs tested achieved steady EC_{50} values within 36 hours equivalent to those observed at 48 hours (Fig 8E). These results indicate that the active AKI drugs achieve their anti-amoebic effects as rapidly as the current treatment, metronidazole.

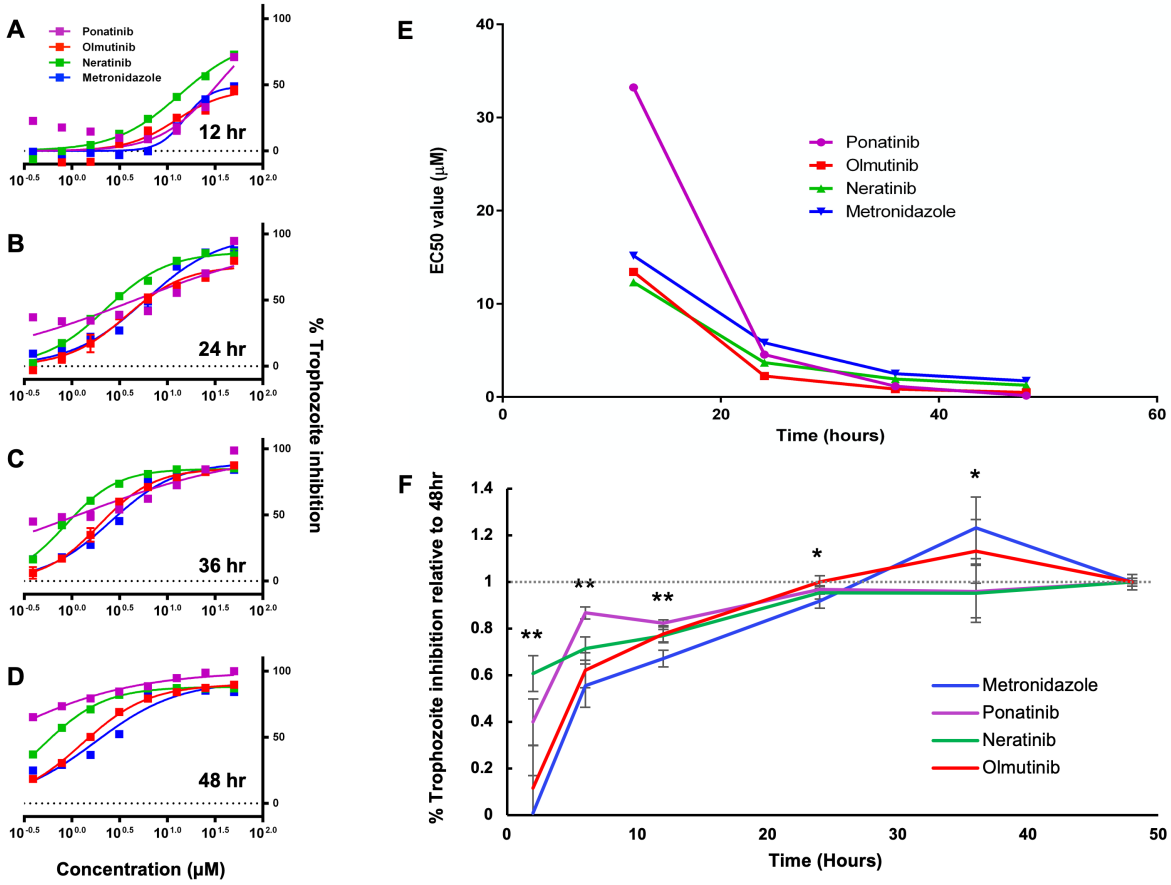

Figure 1.8 Timing of drug action against *E. histolytica* trophozoites.
(A - D) Dose-response curves measured at 12, 24, 36, and 48hr for ponatinib, neratinib, olmutinib, and metronidazole. (E) Plot of EC_{50} values calculated from the data shown in (A-D) graphed over time. (F) Plot of *E. histolytica* trophozoite inhibition by AKI drugs after varying exposure times. Trophozoites were treated with ponatinib, neratinib, olmutinib, or metronidazole at 5μM for 2, 6, 12, 24, 36, or 48hr, followed by drug washout and continued incubation until 48hr. Percent inhibition was then determined. Points represent % inhibition for each drug and exposure time scaled to the 48hr % inhibition value for the same drug. Statistical difference between groups was determined by 1-way ANOVA for each exposure time. (** = $p < 0.01$) (* = $p < 0.05$)

Hit compounds and metronidazole require similar exposure times for *E. histolytica* trophozoite inhibition

To determine the amount of exposure time necessary for parasite killing by the compounds most active in the initial and extended screens, *E. histolytica* trophozoite inhibition was measured following varying treatment periods with either ponatinib, neratinib, olmutinib, or metronidazole. Cells were treated with drugs at 5 μM for intervals ranging from 2 to 48 hours, followed by drug washout and continued incubation to 48 total hours. This concentration was chosen to ensure complete parasite killing by all drugs after 48 hours. Trophozoite viability was measured for each drug and exposure time using CellTiter-glo and the percentage inhibition was calculated. Because each drug tested possess a different anti-amoebic EC_{50} value, the percentage inhibition for each exposure time was scaled to the 48-hour value for each respective drug. As a result, the relative effectiveness of varying exposure times could be compared across drugs irrespective of varying drug potency. All drug treatments achieved inhibition levels after 24 hours of exposure time similar to levels observed after 48 hours (Fig 8F). These results indicate that ponatinib, neratinib, olmutinib, and metronidazole all require roughly 24 hours of parasite exposure time in order to achieve maximal levels of parasite inhibition. Additionally, both ponatinib and neratinib achieved significantly higher scaled % inhibition levels after 2, 6, and 12 hours compared to metronidazole, indicating that a somewhat shorter exposure time might be required for these drugs to achieve their antiparasitic effects.

Antineoplastic kinase inhibitors kill mature *Entamoeba* cysts

A major drawback of metronidazole as a treatment for amebiasis is its poor activity against luminal parasites and cysts [2]. To determine if AKIs may be superior in this respect, we assayed for killing of mature *Entamoeba* cysts. As *E. histolytica* cannot be induced to encyst *in vitro* [21], the related

parasite, *E. invadens*, a well-characterized model system for *Entamoeba* development, was utilized. Mature (72h) cysts of a transgenic line constitutively expressing luciferase were treated with 10 μM dasatinib, bosutinib, ibrutinib, or 0.5% DMSO as negative control, for 3 days. After treatment, cysts were treated with distilled water for five hours to remove any remaining trophozoites, and luciferase activity was assayed. Ibrutinib was found to significantly reduce luciferase signal to between 10% and 50% of controls, indicating that this AKI drug is capable of killing *Entamoeba* cysts. In contrast, metronidazole up to 20 μM had no effect (Fig 9). As ibrutinib is known to act as a covalent inhibitor of human kinase proteins, another such covalent inhibitor which showed activity in the extended screen, acalabrutinib, was also tested [22, 23]. However, this drug did not consistently display any significant cysticidal activity.

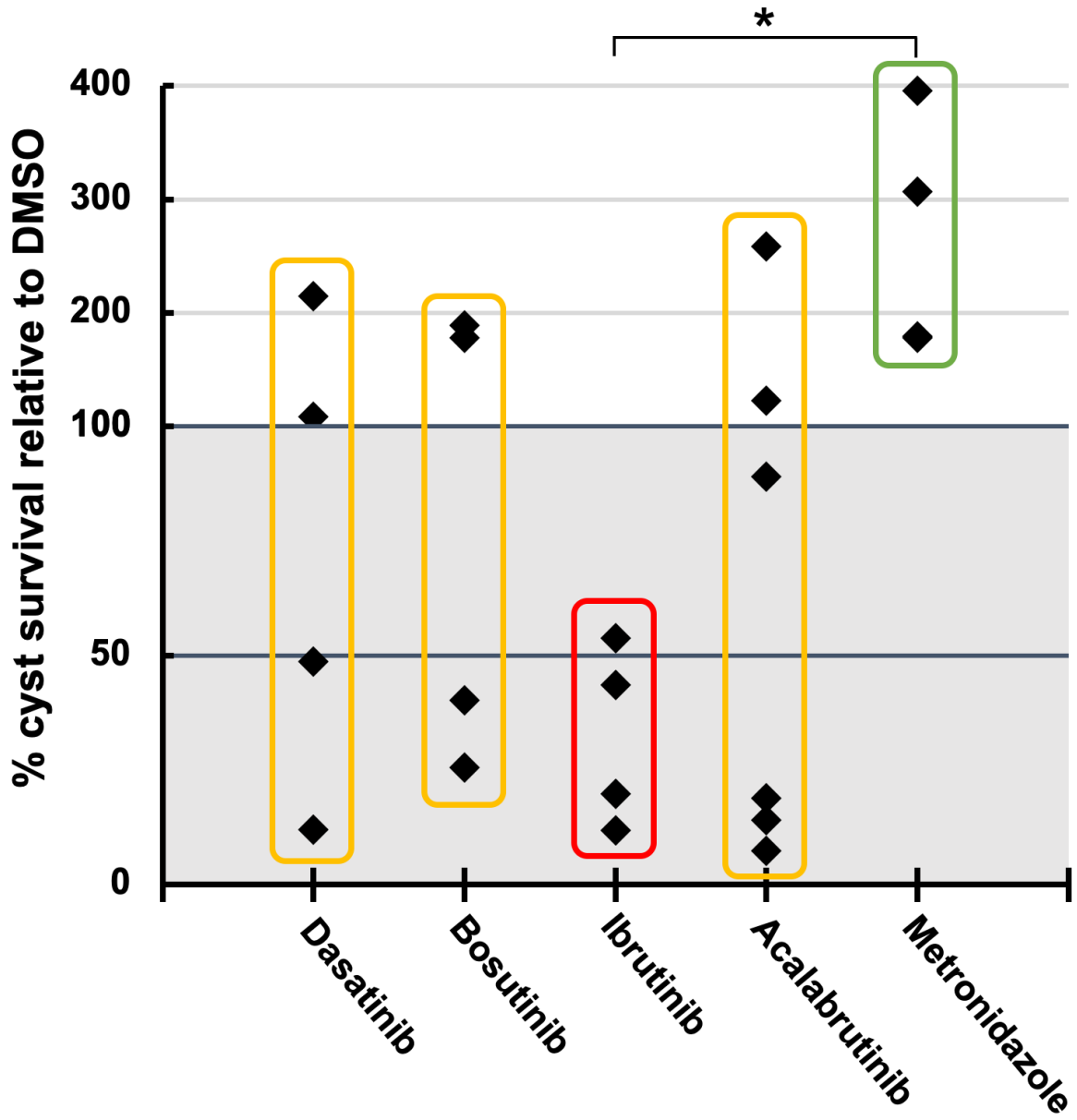

Figure 1.9 Activity of antineoplastic kinase inhibitors against *Entamoeba* cysts.
Cyst survival measured using luminescence values of luciferase-expressing *E. invadens* cysts after drug treatments, compared with DMSO-treated controls. Cysticidal effect corresponds to cyst survival values below 100%. Metronidazole tested at 20µM. All other drugs tested at 10µM. Data points represent biological replicates. Asterisk indicates ($p < 0.05$).

Discussion

Treatment options for amoebiasis are currently limited to either nitroimidazole drugs such as metronidazole, which acts via anaerobic activation to toxic reactive forms in *E. histolytica* [10]. While other drugs have been proposed or used at times, a 2013 systematic review concluded that only nitroimidazole drugs and the thiazolide drug nitazoxanide are likely to be beneficial to patients [10]. This fact, when coupled with emerging drug resistance to metronidazole as well as its lack of activity against the infectious cyst form of *E. histolytica* necessitates the search for new treatment options [13].

In this study we tested the hypothesis that *E. histolytica* could be killed by FDA-approved antineoplastic kinase inhibitors, possibly via action on parasitic homologs of human kinases. Out of 24 such drugs tested, six were shown to possess strong anti-amoebic properties, representing a completely new class of drugs in this area. All of the six highly active drugs displayed unique and important advantages over the current treatment. Dasatinib, ibrutinib, bosutinib, ponatinib, neratinib, and olmutinib were all for the first time shown to kill *E. histolytica* trophozoites *in vitro* significantly more potently than metronidazole. Ponatinib, neratinib, and olmutinib in particular demonstrated sub-micromolar EC_{50} values rarely observed for any compound against this organism. These latter three were also shown to act as rapidly as metronidazole, and two of them, ponatinib and neratinib, were shown to act after shorter exposure times. Significantly, ibrutinib was also shown to kill the cysts of the related model organism *E. invadens* in contrast to metronidazole which did not. This feature is particularly unique and desirable for epidemiological purposes. Outside of the current study, both ibrutinib and neratinib have been shown to possess good brain penetrance, as does metronidazole [24-26]. Taken together all these properties give the six drugs strong potential for repurposing against *E. histolytica* infection, especially in advanced

amoebiasis cases where infection has progressed to the liver or brain, or in cases of cancer patients with *E. histolytica* infections [3, 8, 27].

Interestingly, a recent high-throughput screen of the reframeDB commercial drug library also observed activity of ponatinib and dasatinib against *E. histolytica*, as well as the tyrosine kinase inhibitor rebastinib not included in the current study. While this screen is currently unpublished, the results can be viewed at (https://reframedb.org/assays/A00203). The researchers involved in this screen have also conducted screens of the same library against the parasitic amoebae *Naegleria fowleri* and *Balamuthia mandrillaris*, both of which found ponatinib to be active [28]. All of these results further validate the potential for AKIs as a new class of highly potent drugs against *E. histolytica*, and potentially other parasitic amoeba as well.

One aspect of AKIs which is highly relevant to their potential for use as an amoebiasis treatment is adverse effects. All 6 of the drugs found to be highly active in this study are known to produce notable adverse effects, especially given the weeks-long dosing regimens often employed in cancer chemotherapy [29-38]. While a wide range of adverse effects have been observed, of particular concern in this case would be those which overlap with the symptoms of amoebiasis itself, such as diarrhea and other gastrointestinal effects [2]. Such an overlap between disease symptoms and drug adverse effects already exists with metronidazole, and due to its potential to reduce patient therapeutic compliance, would best be avoided in the development of any future treatments against this disease [7]. As such, the AKI drugs found to be active in this study can be ranked based on the nature of their most common adverse effects, with priority given to those with the lowest observed overlap with amoebiasis symptoms. A literature search on this topic revealed relevant studies for all of the 6 active AKI drugs discussed in this study, including safety and adverse reaction data for single or double doses in healthy subjects [39-47]. As can be observed from the summary of this data in Table 3, out of the 6 drugs, only dasatinib and ponatinib

had few-to-no gastrointestinal adverse reactions, rendering these two drugs the most promising candidates of the 6 for further development against amoebiasis.

Table 1.4 A selection of published data regarding the adverse effects of 1-2 doses of AKI drugs of interest in healthy subjects.

Drug name	Most frequent adverse reactions	Dosing	Reference
Dasatinib	Headache	2 doses, 50mg	(Eley *et al*., 2009) [40]
Ibrutinib	Abdominal pain, diarrhea, headache	1 dose, 140mg	(Scheers *et al*., 2014) [41]
Bosutinib	Diarrhea, decreased by administering with food	1 dose, 200-800mg	(Abbas *et al*., 2012) [39]
Ponatinib	No significant adverse reactions	1 dose, 45mg	(Narasimhan *et al*., 2015) [45]
Ponatinib	Headache, increased lipase	1 dose, 45mg	(Narasimhan *et al*., 2013) [47]
Ponatinib	Nausea	1 dose, 30mg	(Narasimhan *et al*., 2014) [46]
Ponatinib	Headache, increased lipase levels	1 dose, 45mg	(Narasimhan *et al*., 2014) [44]
Neratinib	Gastrointestinal adverse events	1 dose, 240mg	(Abbas *et al*., 2011) [42]
Olmutinib	Diarrhea and oropharyngeal pain	1 dose, 100-300mg	(Noh *et al*., 2019) [43]

Another important consideration for the potential of these drugs to be developed as amoebiasis treatments is their pharmacokinetic properties. Most critically, the questions to be answered are: whether these drugs reach therapeutically relevant concentrations in the bloodstream, how long it takes for them to reach those concentrations, and for what length of time do they remain in the bloodstream in measurable amounts? These three questions can be answered by data regarding the C_{max} (maximum blood plasma concentration), T_{max} (time to reach maximum plasma concentration), and $T_{1/2}$ (plasma half-life) metrics for each drug. A search of available literature on this topic is summarized in Table 4 [39-47]. As can be seen in Table 4, ponatinib has been observed in multiple studies to reach plasma concentrations close to its EC_{50} value of 129.9nM against *E. histolytica* following single 45mg doses. Additionally, ponatinib's observed half-life in these same studies ranged from 24-36 hours. Given ponatinib's relatively mild and largely non-gastrointestinal adverse effects at these same doses, these observations raise the possibility of ponatinib being effective in treatment against amoebiasis using a low number of total doses. Such a minimal dosing strategy could potentially have the benefits of both reducing total adverse effects experienced by patients well below those observed in long-term cancer chemotherapy scenarios, as well as reducing the overall complexity of the therapeutic regimen. This in turn could potentially increase patient compliance, thus reducing opportunities for recrudescence and disease spread.

Taken together the results of this study presented here document a new class of FDA-approved drugs with strong potential for repurposing against a widespread and devastating pathogen. Future research may expand on these findings by characterizing the molecular mechanisms underlying the actions of these drugs as well as testing their *in vivo* efficacy.

Table 1.5 Published pharmacokinetic data for AKI drugs of interest following 1-2 doses in healthy subjects.

Drug name	Dosing & subjects	Cmax (nM)	Tmax (hr)	T1/2 (hr)	Reference
Dasatinib	2 doses, 50mg	90	1	<10	(Eley *et al*., 2009) [40]
Ibrutinib	1 dose, 140mg	80	0.5	3.33	(Scheers *et al*., 2014) [41]
Bosutinib	1 dose, 200-800mg	30-410	6	32-41	(Abbas *et al*., 2012) [39]
Ponatinib	1 dose, 45mg	110	6	27	(Narasimhan *et al*., 2015) [45]
Ponatinib	1 dose, 45mg	100	6	24	(Narasimhan *et al*., 2013) [47]
Ponatinib	1 dose, 30mg	80	5	36	(Narasimhan *et al*., 2014) [46]
Ponatinib	1 dose, 45mg	100	5	24	(Narasimhan *et al*., 2014) [44]
Neratinib	1 dose, 240mg	100	6	11	(Abbas *et al*., 2011) [42]
Olmutinib	1 dose, 100-300mg	2240-3070	2.5-3	6	(Noh *et al*., 2019) [43]

Materials and Methods

E. histolytica cell culture

E. histolytica strain HM-1:IMSS trophozoites were maintained in 50ml culture flasks (Greiner Bio-One) containing TYI-S-33 media, 10% heat-inactivated adult bovine serum (Sigma), 1% MEM Vitamin Solution (Gibco), supplemented with penicillin (100 U/mL) and streptomycin (100 μg/mL) (Omega Scientific) [14].

Compounds

Compounds for screens were purchased from Fisher Scientific and Millipore-Sigma.

Cell viability screen to determine drug potency against *E. histolytica*

Following a previously-published approach [14] *E. histolytica* trophozoites maintained in the logarithmic phase of growth were seeded into 96-well plates (Greiner Bio-One) at 5,000 cells/well to a total volume of 100 μl/well. 8- or 16-point two-fold dilution series of the treatment compounds were prepared, beginning at a maximum final treatment concentration of 50 μM. 0.5 μl of each drug concentration was added to triplicate wells for each treatment group. 0.5 μl of DMSO was used as a negative control, and 0.5 μl of 10 mM metronidazole dissolved in DMSO was used as a positive control, giving a final concentration of 50 μM. Alternatively, wells with only media were used as a negative control. The plates were placed in GasPak EZ (Becton-Dickinson) bags and incubated at 37°C for 48hr. Plates were removed and 50 μl of CellTiter-Glo (Promega) was added to each well. Plates were shaken and incubated in darkness for 20 minutes and the luminescence value of each well was read by a luminometer (EnVision, PerkinElmer). Percent inhibition was calculated by subtracting the luminescence

values of each experimental data point from the average minimum signal obtained from positive control values and dividing by the difference between the average maximum signal negative control and the positive control. The resulting decimal value was then multiplied by 100 to give a percentage.

Determination of drug EC_{50} values *in vitro* over time

Effects of different concentrations of compounds on *E. histolytica* trophozoite cell viability were determined as described in the previous section at a series of timepoints ranging from 6 hours to 48 hours following drug administration. EC_{50} values were calculated at each timepoint as previously described.

Determination of varying drug exposure time effects

E. histolytica trophozoites were treated with either 5μM ponatinib, 5μM neratinib, 5μM olmutinib, or 10μM metronidazole in replicates of 4 wells in 96-well plates. At timepoints ranging from 2 to 48 hours, wells were aspirated, washed once with fresh media, and refilled with fresh media. At 48 hours, percentage trophozoite inhibition was measured using luminescence and calculated as described previously for each timepoint.

Identification of desired target profile of active drugs

A desired target profile of active drugs was generated using the "Multi-drug target finder" tool in the CancerDrugMap (http://ruben.ucsd.edu/dnet/maps/drug_find.html) [20]. Drugs that were active (dasatinib, bosutinib, ibrutinib...) and inactive (nilotinib, imatinib...) in the *E. histolytica* proliferation assay were inputs, respectively. Drug-target interaction activity data for the tool were collected from multiple sources as previously described, including ChEMBL, PubChem, and literature sources [20]. Drug targets were ranked based on the drug-target activity data and using the following equations and

assembled into the final anti-amoebic activity-associated profile.

$$Score\ of\ target\ S = \sum_{drugs} weight \times (pAct - 4)$$

Where

$$pAct\ = -log(\ IC50/Kd/Ki\ )$$

For active drugs: $weight = 1$

For inactive drugs: $weight\ = -0.6 \times \sqrt{\frac{number\ of\ active\ drugs}{number\ of\ inactive\ drugs}}$

Identification of drugs with desired target profile

A list of drugs with target profiles matching the desired target profile was generated with the "Multi-target drug finder" tool in CancerDrugMap (http://ruben.ucsd.edu/dnet/maps/tar_find.html). The desired target profiles generated above were input correspondingly. Resulting cancer drugs were ranked based on the drug-target activity and the following equations.

$$Score\ of\ drug\ S = \sum_{target} weight \times (pAct - 4)$$

Where

$$pAct\ = -log(\ IC50/Kd/Ki\ )$$

For targets to hit: $weight = 1$

For targets to avoid: $weight\ = -0.6 \times \sqrt{\frac{number\ of\ wanted\ targets}{number\ of\ unwanted\ targets}}$

Top-ranking drugs were then selected for further testing.

Identification of potential targets of active drugs in the *E. histolytica* genome

15 top ranking human protein targets (YES1, ABL1, BTK, BMX, LCK, HCK, FGR, BLK, ERBB4, LYN, FYN, SRC, CSK, ABL2, and FRK) from the identified desired target profile were searched against the *E. histolytica* genome downloaded from (https://amoebadb.org/common/downloads/Current_Release/EhistolyticaHM1IMSS/). Human protein sequences were downloaded from (uniprot.org) and the annotated kinase domains of each protein were compiled into a single file. Full gapped optimal sequence alignments with zero end gap penalties (ZEGA) were performed between the kinase domain sequences of the 15 targets and the *E. histolytica* genome. The significance of each alignment was assessed according to a number of residue substitution matrices as a pP value (pP = -log(P-value)) [48]. *E. histolytica* genes with pP over 10, namely the P-value of the alignment lower than 10^{-10} were selected as potential targets. A network map of the 15 top ranking human genes and homologous *E. histolytica* genes was generated with Graphviz neato, with edges corresponding to the pP values between human and *E. histolytica* genes.

Cyst killing assay

For assays on mature cysts, a transgenic *E. invadens* line stably expressing luciferase (CK-luc) was used [49]. Mature cyst viability assay was performed as described previously [16]. Parasites were induced to encyst by incubation in encystation media (47% LG) [21]. After 72 h, parasites were washed once in distilled water and incubated at 25°C for 4-5 h in water to lyse trophozoites. Purified cysts were pelleted, counted to ensure equal cyst numbers, and resuspended in encystation media at a concentration of 1-5x10^5 cells per ml. One ml suspension per replicate was transferred to glass tubes containing encystation media and drug or DMSO, then incubated at 25°C for 72 h. On the day of the assay, cysts were pelleted and treated once more with distilled water for 5 h to lyse any trophozoites that had emerged during treatment. Purified cysts were then resuspended in 75 µl Cell Lysis buffer (Promega) and

sonicated for 2x10 seconds to break the cyst wall. Luciferase assay was performed using the Promega luciferase assay kit according to the manufacturer's instructions. Assays were performed on equal volume of lysate (35 µl) and not normalized to protein content. Effect of the drug was calculated by comparison to DMSO control, after subtraction of background signal. Significance of drug effects was calculated using a one-tailed T-test.

Funding acknowledgments

This work was supported in part by NIH grant R21AI146460. C.S. was supported by the University of California San Diego Global Health Institute graduate student research grant 2017-2018. G.E. received funding from the SPARK Translational Research Program at Stanford University, the United States National Institute of Health grant R21-AI123594, and the United States National Institute of Health National Center for Advancing Translational Science grant UL1-TR001085. D.S. and A.D. received funding from the United States National Institute of Health grant 1KL2TR001444. R.A. received funding from the United States National Institute of Health National Institute of General Medical Sciences grant GM071872.

Author Contributions

Conceptualization, C.S., R.A.; Methodology, C.S., G.E., D.S., A.D.; Formal Analysis, C.S.; Data Curation, C.S.; Writing – Original Draft, C.S.; Visualization, C.S.; Supervision, R.A., A.D. ; Funding Acquisition, R.A.; Writing – review & editing, C.S., G.E., D.S., A.D., and R.A.; Software, D.S.

Conflicts of Interest

The authors have no conflicts of interest.

Chapter 1, in part, is a reprint of the material as it may appear in PLOS Neglected Tropical Diseases, 2021, Conall Sauvey, Gretchen Ehrenkaufer, Da Shi, Anjan Debnath, Ruben Abagyan. The dissertation author was the primary investigator and author of this paper.

References

1. Shirley DT, Farr L, Watanabe K, Moonah S. A Review of the Global Burden, New Diagnostics, and Current Therapeutics for Amebiasis. Open forum infectious diseases. 2018;5(7):ofy161.

2. Pritt BS, Clark CG. Amebiasis. Mayo Clin Proc. 2008;83(10):1154-9; quiz 9-60.

3. Ralston KS, Petri WA, Jr. Tissue destruction and invasion by Entamoeba histolytica. Trends in parasitology. 2011;27(6):254-63.

4. Faria CP, Zanini GM, Dias GS, da Silva S, de Freitas MB, Almendra R, Santana P, Sousa MD. Geospatial distribution of intestinal parasitic infections in Rio de Janeiro (Brazil) and its association with social determinants. PLoS Negl Trop Dis. 2017;11(3):e0005445.

5. Sahimin N, Lim YA, Ariffin F, Behnke JM, Lewis JW, Mohd Zain SN. Migrant Workers in Malaysia: Current Implications of Sociodemographic and Environmental Characteristics in the Transmission of Intestinal Parasitic Infections. PLoS Negl Trop Dis. 2016;10(11):e0005110.

6. Verkerke HP, Petri WA, Jr., Marie CS. The dynamic interdependence of amebiasis, innate immunity, and undernutrition. Semin Immunopathol. 2012;34(6):771-85.

7. Dusengeyezu E, Kadima J. How do Metronidazole Drawbacks Impact Patient Compliance and Therapeutic Outcomes in Treating Amoebiasis in Rwanda. International Journal of TROPICAL DISEASE & Health. 2016;17(3):1-7.

8. Carrero JC, Reyes-Lopez M, Serrano-Luna J, Shibayama M, Unzueta J, Leon-Sicairos N, de la Garza M. Intestinal amoebiasis: 160 years of its first detection and still remains as a health problem in developing countries. Int J Med Microbiol. 2020;310(1):151358.

9. Garduno-Espinosa J, Martinez-Garcia MC, Fajardo-Gutierrez A, Ortega-Alvarez M, Alvarez-Espinosa A, Vega-Perez V, Munoz-Hernandez O. Frequency and risk factors associated with metronidazole therapeutic noncompliance. Revista de investigacion clinica; organo del Hospital de Enfermedades de la Nutricion. 1992;44(2):235-40.

10. Marie C, Petri WA, Jr. Amoebic dysentery. BMJ clinical evidence. 2013;2013.

11. Kikuchi T, Koga M, Shimizu S, Miura T, Maruyama H, Kimura M. Efficacy and safety of paromomycin for treating amebiasis in Japan. Parasitology international. 2013;62(6):497-501.

12. Blessmann J, Tannich E. Treatment of asymptomatic intestinal Entamoeba histolytica infection. The New England journal of medicine. 2002;347(17):1384.

13. Wassmann C, Hellberg A, Tannich E, Bruchhaus I. Metronidazole resistance in the protozoan parasite Entamoeba histolytica is associated with increased expression of iron-containing superoxide

dismutase and peroxiredoxin and decreased expression of ferredoxin 1 and flavin reductase. The Journal of biological chemistry. 1999;274(37):26051-6.

14. Debnath A, Parsonage D, Andrade RM, He C, Cobo ER, Hirata K, Chen S, Garcia-Rivera G, Orozco E, Martinez MB, Gunatilleke SS, Barrios AM, Arkin MR, Poole LB, McKerrow JH, Reed SL. A high-throughput drug screen for Entamoeba histolytica identifies a new lead and target. Nat Med. 2012;18(6):956-60.

15. Bashyal B, Li L, Bains T, Debnath A, LaBarbera DV. Larrea tridentata: A novel source for anti-parasitic agents active against Entamoeba histolytica, Giardia lamblia and Naegleria fowleri. PLoS Negl Trop Dis. 2017;11(8):e0005832.

16. Ehrenkaufer GM, Suresh S, Solow-Cordero D, Singh U. High-Throughput Screening of Entamoeba Identifies Compounds Which Target Both Life Cycle Stages and Which Are Effective Against Metronidazole Resistant Parasites. Front Cell Infect Microbiol. 2018;8:276.

17. Mi-Ichi F, Ishikawa T, Tam VK, Deloer S, Hamano S, Hamada T, Yoshida H. Characterization of Entamoeba histolytica adenosine 5'-phosphosulfate (APS) kinase; validation as a target and provision of leads for the development of new drugs against amoebiasis. PLoS Negl Trop Dis. 2019;13(8):e0007633.

18. Nurkanto A, Jeelani G, Yamamoto T, Naito Y, Hishiki T, Mori M, Suematsu M, Shiomi K, Hashimoto T, Nozaki T. Characterization and validation of Entamoeba histolytica pantothenate kinase as a novel anti-amebic drug target. Int J Parasitol Drugs Drug Resist. 2018;8(1):125-36.

19. Anamika K, Bhattacharya A, Srinivasan N. Analysis of the protein kinome of Entamoeba histolytica. Proteins. 2008;71(2):995-1006.

20. Capparelli EV, Bricker-Ford R, Rogers MJ, McKerrow JH, Reed SL. Phase I Clinical Trial Results of Auranofin, a Novel Antiparasitic Agent. Antimicrob Agents Chemother. 2017;61(1).

21. Shi D, Khan F, Abagyan R. Extended Multitarget Pharmacology of Anticancer Drugs. J Chem Inf Model. 2019;59(6):3006-17.

22. Sanchez L, Enea V, Eichinger D. Identification of a developmentally regulated transcript expressed during encystation of Entamoeba invadens. Mol Biochem Parasitol. 1994;67(1):125-35.

23. Barf T, Covey T, Izumi R, van de Kar B, Gulrajani M, van Lith B, van Hoek M, de Zwart E, Mittag D, Demont D, Verkaik S, Krantz F, Pearson PG, Ulrich R, Kaptein A. Acalabrutinib (ACP-196): A Covalent Bruton Tyrosine Kinase Inhibitor with a Differentiated Selectivity and In Vivo Potency Profile. J Pharmacol Exp Ther. 2017;363(2):240-52.

24. Davids MS, Brown JR. Ibrutinib: a first in class covalent inhibitor of Bruton's tyrosine kinase. Future Oncol. 2014;10(6):957-67.

25. Bradley CA. Brain metastases respond to neratinib plus capecitabine. Nature reviews Clinical oncology. 2019;16(6):336.

26. Goldwirt L, Beccaria K, Ple A, Sauvageon H, Mourah S. Ibrutinib brain distribution: a preclinical study. Cancer chemotherapy and pharmacology. 2018;81(4):783-9.

27. Duchnowska R, Loibl S, Jassem J. Tyrosine kinase inhibitors for brain metastases in HER2-positive breast cancer. Cancer treatment reviews. 2018;67:71-7.

28. Petri WA, Haque R. Entamoeba histolytica brain abscess. Handbook of clinical neurology. 2013;114:147-52.

29. Kangussu-Marcolino MM, Ehrenkaufer GM, Chen E, Debnath A, Singh U. Identification of plicamycin, TG02, panobinostat, lestaurtinib, and GDC-0084 as promising compounds for the treatment of central nervous system infections caused by the free-living amebae Naegleria, Acanthamoeba and Balamuthia. Int J Parasitol Drugs Drug Resist. 2019;11:80-94.

30. Kantarjian HM, Cortes JE, Kim DW, Khoury HJ, Brummendorf TH, Porkka K, Martinelli G, Durrant S, Leip E, Kelly V, Turnbull K, Besson N, Gambacorti-Passerini C. Bosutinib safety and management of toxicity in leukemia patients with resistance or intolerance to imatinib and other tyrosine kinase inhibitors. Blood. 2014;123(9):1309-18.

31. Kaur V, Swami A. Ibrutinib in CLL: a focus on adverse events, resistance, and novel approaches beyond ibrutinib. Ann Hematol. 2017;96(7):1175-84.

32. Dorer DJ, Knickerbocker RK, Baccarani M, Cortes JE, Hochhaus A, Talpaz M, Haluska FG. Impact of dose intensity of ponatinib on selected adverse events: Multivariate analyses from a pooled population of clinical trial patients. Leuk Res. 2016;48:84-91.

33. Ottmann O, Saglio G, Apperley JF, Arthur C, Bullorsky E, Charbonnier A, Dipersio JF, Kantarjian H, Khoury HJ, Kim DW, Healey D, Strauss L, Cortes JE. Long-term efficacy and safety of dasatinib in patients with chronic myeloid leukemia in accelerated phase who are resistant to or intolerant of imatinib. Blood cancer journal. 2018;8(9):88.

34. Caldemeyer L, Dugan M, Edwards J, Akard L. Long-Term Side Effects of Tyrosine Kinase Inhibitors in Chronic Myeloid Leukemia. Curr Hematol Malig Rep. 2016;11(2):71-9.

35. Heiblig M, Rea D, Chretien ML, Charbonnier A, Rousselot P, Coiteux V, Escoffre-Barbe M, Dubruille V, Huguet F, Cayssials E, Hermet E, Guerci-Bresler A, Ame S, Sackmann-Sala L, Roy L, Sobh M, Morisset S, Etienne G, Nicolini FE. Ponatinib evaluation and safety in real-life chronic myelogenous leukemia patients failing more than two tyrosine kinase inhibitors: the PEARL observational study. Exp Hematol. 2018;67:41-8.

36. Tao Z, Li SX, Shen K, Zhao Y, Zeng H, Ma X. Safety and Efficacy Profile of Neratinib: A Systematic Review and Meta-Analysis of 23 Prospective Clinical Trials. Clin Drug Investig. 2019;39(1):27-43.

37. Paydas S. Management of adverse effects/toxicity of ibrutinib. Crit Rev Oncol Hematol. 2019;136:56-63.

38. Irvine E, Williams C. Treatment-, patient-, and disease-related factors and the emergence of adverse events with tyrosine kinase inhibitors for the treatment of chronic myeloid leukemia. Pharmacotherapy. 2013;33(8):868-81.

39. Liao BC, Lin CC, Lee JH, Yang JC. Update on recent preclinical and clinical studies of T790M mutant-specific irreversible epidermal growth factor receptor tyrosine kinase inhibitors. Journal of biomedical science. 2016;23(1):86.

40. Abbas R, Hug BA, Leister C, Gaaloul ME, Chalon S, Sonnichsen D. A phase I ascending single-dose study of the safety, tolerability, and pharmacokinetics of bosutinib (SKI-606) in healthy adult subjects. Cancer chemotherapy and pharmacology. 2012;69(1):221-7.

41. Eley T, Luo FR, Agrawal S, Sanil A, Manning J, Li T, Blackwood-Chirchir A, Bertz R. Phase I study of the effect of gastric acid pH modulators on the bioavailability of oral dasatinib in healthy subjects. J Clin Pharmacol. 2009;49(6):700-9.

42. Scheers E, Leclercq L, de Jong J, Bode N, Bockx M, Laenen A, Cuyckens F, Skee D, Murphy J, Sukbuntherng J, Mannens G. Absorption, metabolism, and excretion of oral (1)(4)C radiolabeled ibrutinib: an open-label, phase I, single-dose study in healthy men. Drug Metab Dispos. 2015;43(2):289-97.

43. Abbas R, Hug BA, Leister C, Burns J, Sonnichsen D. Pharmacokinetics of oral neratinib during co-administration of ketoconazole in healthy subjects. British journal of clinical pharmacology. 2011;71(4):522-7.

44. Noh YS, Yoon S, Kim SR, Lee KT, Jang IJ. A safety, pharmacokinetic, pharmacogenomic and population pharmacokinetic analysis of the third-generation EGFR TKI, olmutinib (HM61713), after single oral administration in healthy volunteers. Basic Clin Pharmacol Toxicol. 2019;125(4):370-81.

45. Narasimhan NI, Dorer DJ, Davis J, Turner CD, Sonnichsen D. Evaluation of the effect of multiple doses of lansoprazole on the pharmacokinetics and safety of ponatinib in healthy subjects. Clin Drug Investig. 2014;34(10):723-9.

46. Narasimhan NI, Dorer DJ, Davis J, Turner CD, Sonnichsen D. Evaluation of the effect of multiple doses of rifampin on the pharmacokinetics and safety of ponatinib in healthy subjects. Clin Pharmacol Drug Dev. 2015;4(5):354-60.

47. Narasimhan NI, Dorer DJ, Davis J, Turner CD, Marbury TC, Sonnichsen D. Evaluation of pharmacokinetics and safety of ponatinib in subjects with chronic hepatic impairment and matched healthy subjects. Cancer chemotherapy and pharmacology. 2014;74(2):341-8.

48. Narasimhan NI, Dorer DJ, Niland K, Haluska F, Sonnichsen D. Effects of food on the pharmacokinetics of ponatinib in healthy subjects. Journal of clinical pharmacy and therapeutics. 2013;38(6):440-4.

49. Abagyan RA, Batalov S. Do aligned sequences share the same fold? Journal of molecular biology. 1997;273(1):355-68.

50. Ehrenkaufer GM, Singh U. Transient and stable transfection in the protozoan parasite Entamoeba invadens. Mol Biochem Parasitol. 2012;184(1):59-62.

Supporting information

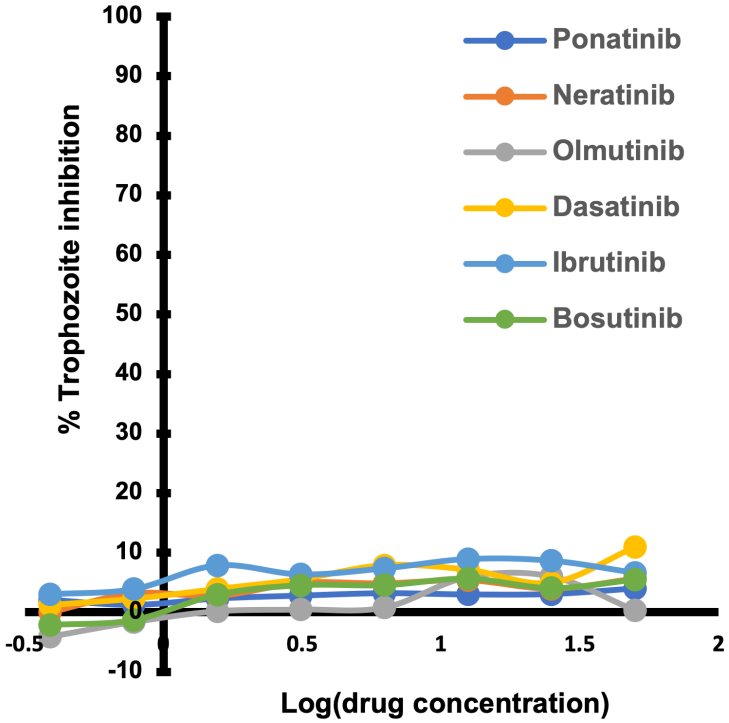

Supplementary figure 1.10 False-positive assay against *E. histolytica* trophozoites.
All drugs were tested at a serially-diluted range of concentrations. Cell viability measured at T = 0.
https://doi.org/10.1371/journal.pntd.0008425.s001

Supplementary dataset 1.1 Figure 1.1 Data.
https://doi.org/10.1371/journal.pntd.0008425.s002
(XLSX)

Supplementary dataset 1.2 Figure 1.6 Data.
https://doi.org/10.1371/journal.pntd.0008425.s003
(XLSX)

Supplementary dataset 1.3 Figure 1.7 Data.
https://doi.org/10.1371/journal.pntd.0008425.s004
(XLSX)

Supplementary dataset 1.4 Figure 1.8 Data.
https://doi.org/10.1371/journal.pntd.0008425.s005
(XLSX)

Supplementary dataset 1.5 Figure 1.9 Data.
https://doi.org/10.1371/journal.pntd.0008425.s006
(XLSX)

Supplementary dataset 1.6 Figure 1.S1 Data.
https://doi.org/10.1371/journal.pntd.0008425.s007
(XLSX)

CHAPTER 2 HIGH-THROUGHPUT PHENOTYPIC SCREEN IDENTIFIES A NEW FAMILY OF POTENT ANTI-AMOEBIC COMPOUNDS

Abstract

Entamoeba histolytica is a disease-causing parasitic amoeba which affects an estimated 50 million people worldwide, particularly in socioeconomically vulnerable populations experiencing water sanitation issues. Infection with *E. histolytica* is referred to as amoebiasis, and can cause symptoms such as colitis, dysentery, and even death in extreme cases. Drugs exist that are capable of killing this parasite, but they are hampered by downsides such as significant adverse effects at therapeutic concentrations, issues with patient compliance, the need for additional drugs to kill the transmissible cyst stage, and potential development of resistance. Past screens of small and medium sized chemical libraries have yielded anti-amoebic candidates, thus rendering high-throughput screening a promising direction for new drug discovery in this area. In this study, we screened a curated 80,000-compound library from Janssen pharmaceuticals against *E. histolytica* trophozoites *in vitro*, and from it identified a highly potent new inhibitor compound. Further experimentation confirmed the activity of this compound, as well as that of several structurally related compounds, originating from both the Janssen Jump-stARter library, and from chemical vendors, thus highlighting a new structure-activity relationship (SAR). In addition, we confirmed that the compound inhibited *E. histolytica* survival as rapidly as the current standard of care and inhibited transmissible cysts of the related model organism *Entamoeba invadens*. Together these results constitute the discovery of a novel class of chemicals with favorable *in vitro* pharmacological properties which may lead to an improved therapy against this parasite and in all of its life stages.

Introduction

Entamoeba histolytica is a parasitic protozoan amoeba that infects the human intestinal tract and causes the diarrheal disease amoebiasis, also known as amoebic colitis [1]. It is estimated to infect around 50 million people globally at any given time, resulting in approximately 50,000 to 70,000 deaths annually, and as such represents a significant problem from a global health perspective [2-4]. It exists in a two-stage life cycle consisting of an environmentally-resistant, infective cyst stage, and a mobile, invasive trophozoite stage. It is transmitted in a characteristic fecal-oral route, where cysts can be ingested from contaminated water or food. Once ingested, cysts pass through to the host intestinal tract where they release trophozoites. Trophozoites feed and multiply, and under certain conditions invade and infect the surrounding host tissues. They can further re-form into cysts which are passed in the host's feces, and potentially onwards to other hosts [3]. Due to this mode of infection, amoebiasis is most widespread in places where fecal contamination of water or food is likely, such as those where water sanitation is insufficient or non-existent. Thus, it most heavily affects and damages populations that are already socioeconomically vulnerable [4-6]. Symptomatic amoebiasis occurs when trophozoites attack the intestinal lining, causing ulceration, and invade the surrounding tissues [7]. Symptoms usually include long-lasting diarrhea progressing to dysentery, as well as generalized abdominal tenderness and fever [1]. In extreme cases infection can spread from the intestinal region to others such as the liver, lungs, or brain [3, 8]. All of these are significantly more dangerous and more likely to result in mortality.

The current standard of care for amoebiasis is the nitroimidazole drug metronidazole, commonly known under the brand name "Flagyl." Metronidazole has seen widespread use against both amoebiasis and other protozoan parasitic diseases since its discovery in the mid-20th century [9]. Despite its successes however, several critical issues exist with metronidazole which render necessary the continued

search for new treatment options. One of these issues is the significant adverse effects that often accompany metronidazole treatment. Several of these adverse effects are similar to the symptoms of amoebiasis itself, such as diarrhea and fever, and can exacerbate the already difficult experience for the patient to the point of intolerability [10]. In fact, a study from a Rwandan group has found these effects to be associated with patient non-compliance with the course of metronidazole treatment, as well as worse clinical outcomes [11]. Another issue with metronidazole is its inability to kill the transmissible cyst stage of *E. histolytica*, necessitating followup treatment with an additional drug such as paromomycin in order to prevent disease spread [12]. This complication and extension of the overall course of treatment could possibly also reduce the likelihood of full patient compliance with the treatment regimen. Beyond these issues, a final concern is the possibility of emergent resistance to metronidazole therapy. While this has yet to be reported in the field, resistant strains of *E. histolytica* are routinely generated in laboratory settings [13-15].

Given these gaps in the effectiveness of metronidazole therapy for amoebiasis, the search for new and additional compounds capable of inhibiting this parasite is ongoing [16]. In particular, several screening efforts of various sizes have been undertaken, and have produced multiple compounds of interest [17, 18]. In (Debnath *et al*., 2012) the authors identified the FDA-approved drug auranofin as an inhibitor of *E. histolytica* trophozoite growth from a screen of the 910-member Iconix drug library. More recently, authors of this current study conducted a low-throughput targeted screen of antineoplastic kinase inhibitor drugs, identifying multiple highly-potent *E. histolytica* inhibitors including the cancer chemotherapy drug ponatinib [19]. Interestingly, another, much larger screen of the 11,948-member ReFRAME library conducted in parallel by authors of this study also identified ponatinib among its potent hits [18].

Given the success of these past screen-based studies, in this study we expanded upon their approach by conducting a high-throughput, semi-automated phenotypic screen of a large chemical library in collaboration with Janssen Pharmaceuticals, Inc. against *E. histolytica, in vitro*. This library, called the Jump-stARter library, consists of 81,664 small molecules selected for their favorable chemical properties for drug development purposes, as well as their structural diversity. The library was designed with these features in order to "jump-start" novel drug discovery efforts and allow for the identification of structures and structural features that are active in a specified context [20-25]. From the screen of this library, we found a highly active compound against *E. histolytica* trophozoites. Further investigation showed similar activity among several structurally-related compounds included in the library, as well as several additional such compounds purchased from commercial vendors. Of these compounds, we found nearly all of them to be non-toxic to a cultured human cell line. We also identified activity of the initial compound against cysts of the related model organism *Entamoeba invadens*, and found it to inhibit *E. histolytica* at the same rate as metronidazole. Together these results show this new compound to be a promising candidate for drug development against amoebiasis.

Results

High-throughput screen of the Jump-stARter library against *E. histolytica* trophozoites *in vitro*

In order to identify new inhibitors of the human parasite *E. histolytica* we established a collaboration with scientists from Janssen Pharmaceuticals, Inc., and from them, obtained a copy of their Jump-stARter chemical library. This library consists of 81,664 small molecules selected by Janssen medicinal chemists for their chemical diversity and optimal physical properties for drug discovery and development efforts [20, 21, 24, 25]. We screened the Jump-stARter library against *E. histolytica* trophozoites in vitro using a semi-automated, high-throughput methodology. Previous screens using this organism have been accomplished using 96-well or 384-well plate formats, but due to the large size of the Jump-stARter library, we developed and utilized a novel 1536-well-plate-based methodology. All compounds in the library were tested at 25μM, and the viability of the parasite cells after incubation for 48 hours was measured with the luciferase-based CellTiter-glo assay. 297 compounds achieved greater than 70% inhibition values and were thus designated as 'hits' and selected for further investigation (Fig 1).

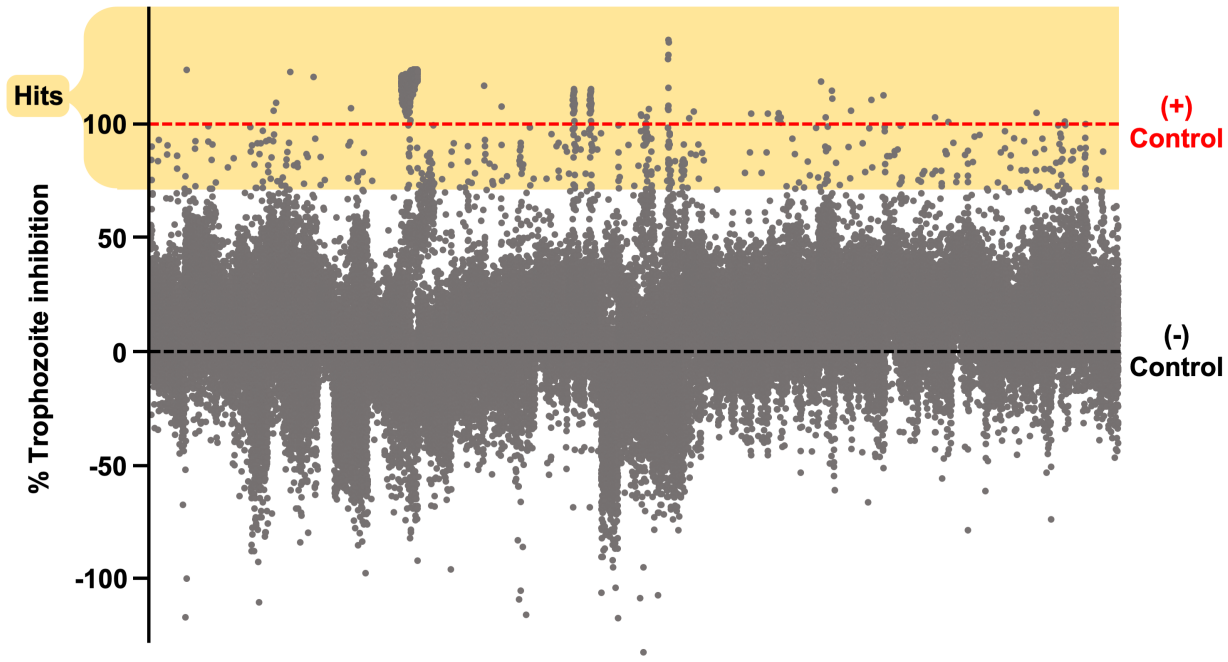

Figure 2.1. High-throughput screening results of 81,664 small molecules against *E. histolytica*. Scatterplot displays percent inhibition values of Jump-stARter library compounds against *E. histolytica* trophozoites calculated relative to positive and negative controls. Grey dots represent individual compound values. Dashed lines represent 0% (average of 10μM Metronidazole, positive controls) and 100% (average of 0.5% DMSO, negative control) percent inhibition values. Yellow box encloses compounds with a percent inhibition value greater than 70%, which were marked as hits and selected for further investigation.

Dose-response screen of top candidate molecules to determine potency

Of the 297 hits from the high-throughput screen, 128 were available to be ordered in additional amounts from Janssen pharmaceuticals. In order to determine their potency, we ordered stock solutions of these compounds and conducted a medium-throughput dose-response screen against *E. histolytica* trophozoites *in vitro*. The compounds were diluted into triplicate 7-point dose-response curves ranging in final assay concentration from 25μM to 0.39μM in a 384-well plate format. Parasite cells were incubated with the compounds, and their viability measured using CellTiter-glo (S2 Dataset). 19 compounds which met the minimum criteria of either producing high levels of parasite inhibition across several points of concentration, or producing a varying range of inhibitions across the different concentrations were selected for further in-depth investigation. Compounds which achieved low or moderate levels of inhibition consistently across all points of concentration were excluded. In order to determine their EC_{50} values, the 19 compounds were tested against *E. histolytica* trophozoites in triplicate 8-point dose response curves in 96-well plates (Fig 2). From these, a compound designated hereafter as JNJ001 achieved the remarkably low EC_{50} value of 0.29μM, with the other compounds achieving values ranging from 4.30μM to 15.72μM (Table 1). These results revealed compound JNJ001 as the top hit, with high inhibitory potency against *E. histolytica* trophozoites.

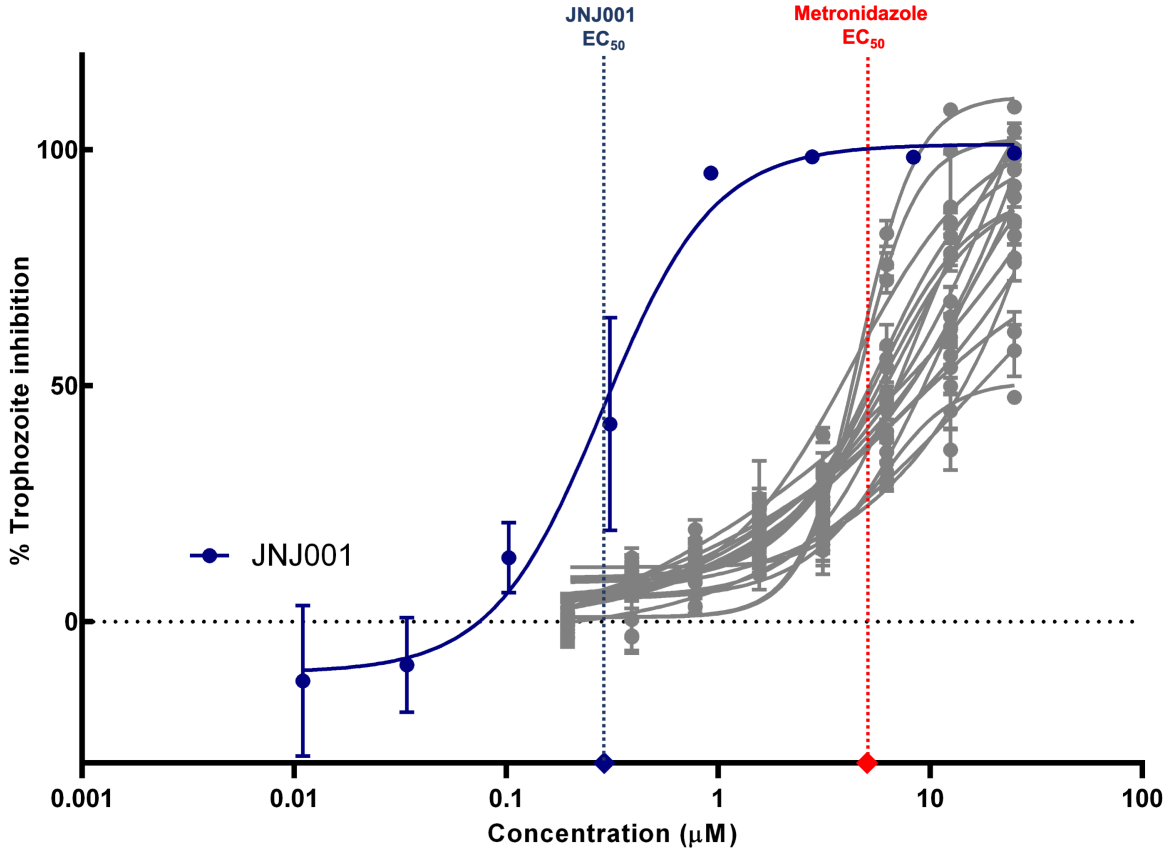

Figure 2.2. EC_{50} determination assay identifies a highly potent inhibitor of *E. histolytica*.
Dose-response curves show percent inhibition of *E. histolytica* trophozoites compared to compound concentration. Trophozoite cell viability was measured after 48 hours of exposure to test compounds, and percent inhibition for each compound was calculated relative to controls. Compound JNJ001 (displayed in dark navy blue) was assayed over a broader range of concentrations compared to other compounds (displayed in grey) due to previous results indicating high potency in lower concentration ranges. Vertical dotted lines represent EC_{50} values of compound JNJ001 (navy blue) and metronidazole (red). Horizontal dotted line represents 0% inhibition level. Error bars represent standard deviation.

Table 2.1 EC_{50} values of top hits from high-throughput screen.

Compound ID:	EC_{50} (µM)
JNJ001	0.29
JNJ002	4.30
JNJ003	4.59
JNJ004	4.59
JNJ005	5.45
JNJ006	5.78
JNJ007	5.78
JNJ008	6.09
JNJ009	6.39
JNJ010	8.37
JNJ011	10.26
JNJ012	10.92
JNJ013	15.72
JNJ014	No effect
JNJ015	No effect
JNJ016	No effect
JNJ017	No effect
JNJ018	No effect
JNJ019	No effect

EC_{50} values determined from dose-response assay against *E. histolytica* trophozoites in vitro. Color scale indicates compound potency. Green = more potent, red = less potent, grey = no effect.

Cell counting assay confirms inhibitory activity against *E. histolytica* trophozoites

In order to confirm the activity of compound JNJ001 against *E. histolytica*, it was once again tested in an 8-point dose-response curve in a 96-well plate, along with metronidazole as a control compound. In this assay however, survival of the parasites was directly determined by cell counting using a hemocytometer. When the results of this assay were plotted alongside the Luciferase-based dose-response curve results, they were found to match closely (Fig 3). This supports the accuracy of the luciferase-based assay results and indicates that compound JNJ001 does in fact act as a potent inhibitor of *E. histolytic*a trophozoites.

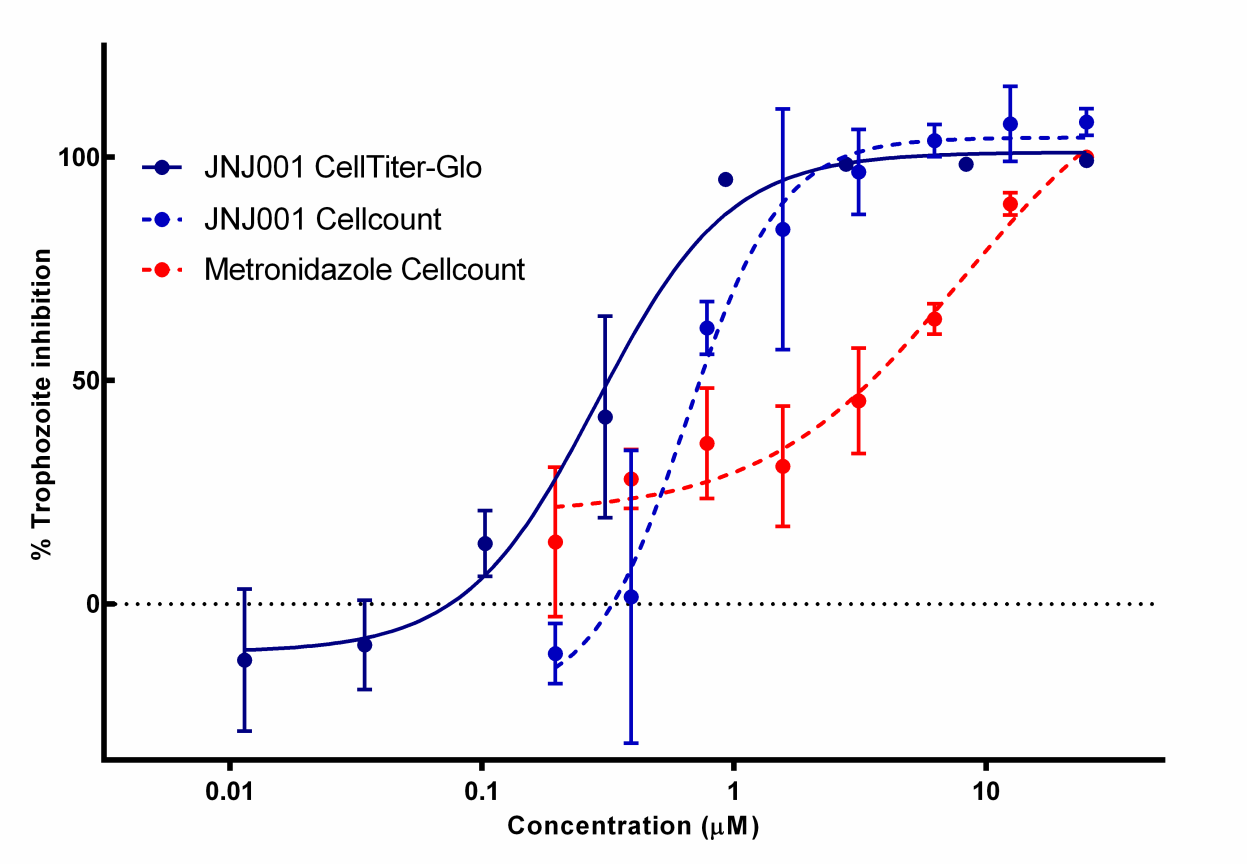

Figure 2.3. Cell counting assay confirms anti-amoebic activity of compound JNJ001.
Dose-response curves show percent inhibition of *E. histolytica* trophozoites compared to compound concentration. Trophozoite cell viability or survival was measured after 48 hours of exposure to test compounds, and percent inhibition for each compound was calculated relative to controls. Dashed lines represent parasite survival measured by cell counting. Solid line represents parasite cell viability measured by a luminescence-based assay. Error bars represent standard deviation.

Human cell toxicity assay

It is a crucial feature of any candidate compound in the drug development process that it not possess toxicity towards human cells, either specifically or as part of a general cytotoxicity. In order to determine whether compound JNJ001 possesses this feature, we tested it for toxicity against human HEK293 cells *in vitro*. In this experiment, human HEK293 cells were cultured and tested in a dose response assay with JNJ001, metronidazole and a selection of antineoplastic kinase inhibitor (AKI) drugs which have previously shown anti-amoebic activity [19]. Of these, only the AKI drug ponatinib produced notable toxicity to the human cells at concentrations up to 25μM, whereas JNJ001, the other AKI drugs, and metronidazole produced no toxicity at all (Fig 4). These results indicate that JNJ001 is both not specifically toxic to human cells and does not inhibit *E. histolytica* due to a generalized cytotoxic mechanism.

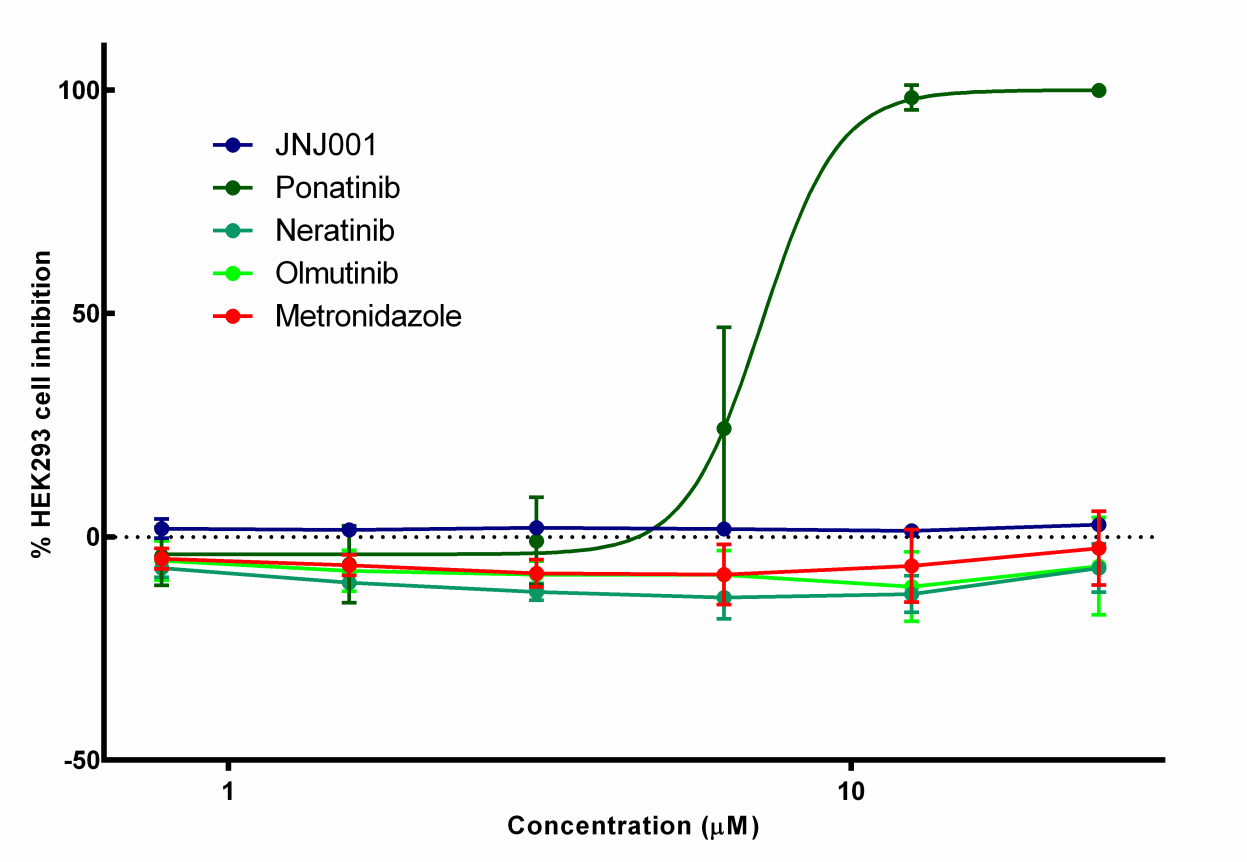

Figure 2.4. Compound JNJ001 does not inhibit human HEK293 cells.
Dose-response curves show percent inhibition of human HEK293 cells compared to compound concentration. Cell viability was measured after 48 hours of exposure to test compounds, and percent inhibition for each compound was calculated relative to positive and negative controls. Compound JNJ001 is represented with a navy blue line. Metronidazole is represented with a red line. Ponatinib is represented with a green line. Error bars represent standard deviation.

Compound JNJ001 inhibits *E. histolytica* as rapidly as metronidazole

In order to determine the speed with which compound JNJ001 achieves its inhibitory potency against *E. histolytica*, we measured and calculated its EC_{50} values at a series of timepoints subsequent to administration, alongside metronidazole for comparison. Cell viability was measured using CellTiter-glo at 12, 24, 36, and 48 hours after the addition of compounds. Both JNJ001 and metronidazole achieved their lowest EC_{50} values between the 24 and 36 hour timepoints (Fig 5), indicating that JNJ001 acts to inhibit *E. histolytica* as rapidly as the current standard of care drug.

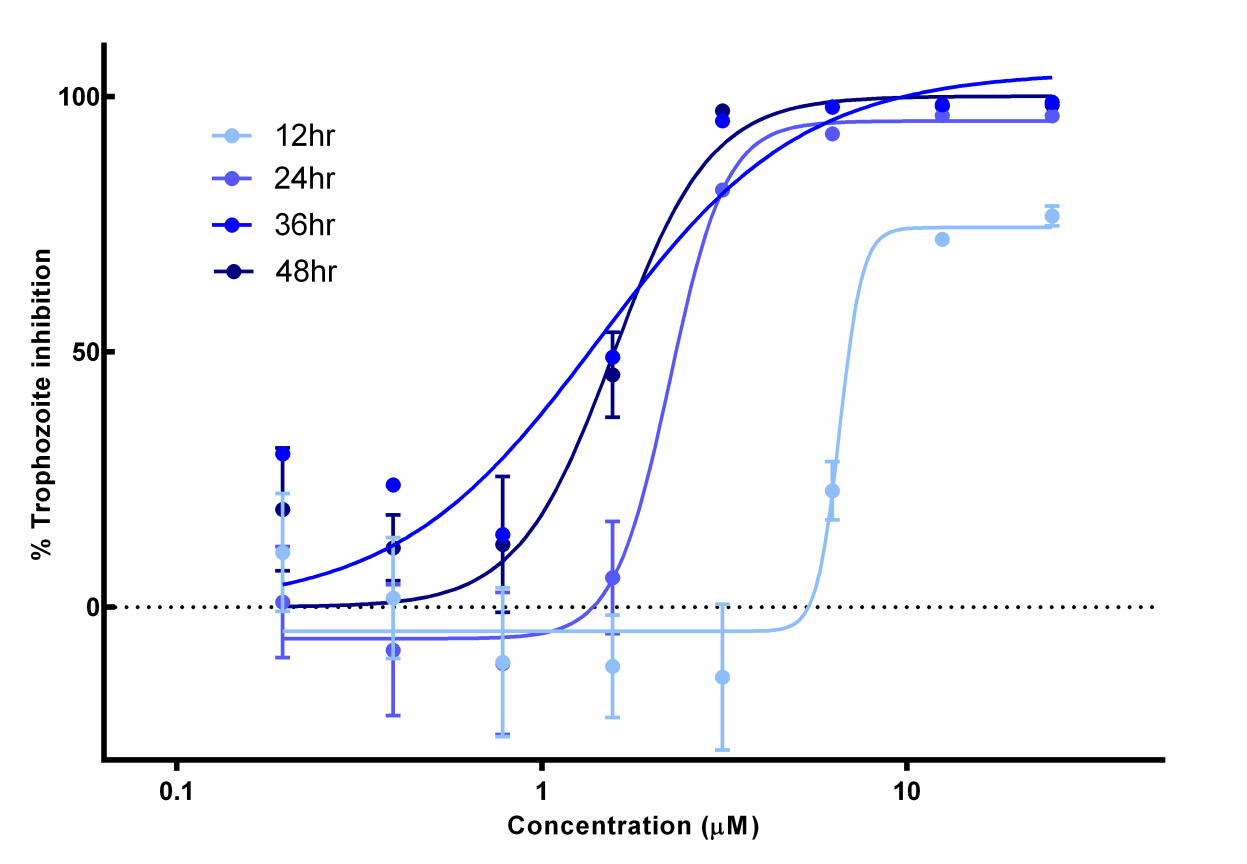

Figure 2.5. Compound JNJ001 achieves peak anti-amoebic effects within 24-36 hours. Dose-response curves show percent inhibition of *E. histolytica* trophozoites compared to compound concentration. Trophozoite cell viability or survival was measured after 12, 24, 36, and 48 hours of exposure to test compounds. Percent inhibition for each data point was calculated relative to average positive and negative control values. Error bars represent standard deviation.

Compound inhibits mature *Entamoeba* cysts

As *E. histolytica* cannot be induced to encyst in vitro, we utilized the related parasite, *E. invadens*, a well-characterized model system for *Entamoeba* development, to assay for inhibition by compound JNJ001 [26]. Mature (72h) cysts of a transgenic line constitutively expressing luciferase were treated with JNJ001 at 10μM or 0.5% DMSO as negative control, for 3 days. After treatment, cysts were treated with distilled water for five hours to remove any remaining trophozoites, and luciferase activity was assayed. JNJ001 was found to reduce luciferase signal compared to controls, indicating that it is capable of killing *Entamoeba* cysts (Fig 6). In contrast, metronidazole up to 20 μM has been previously demonstrated to produce no such inhibition [19].

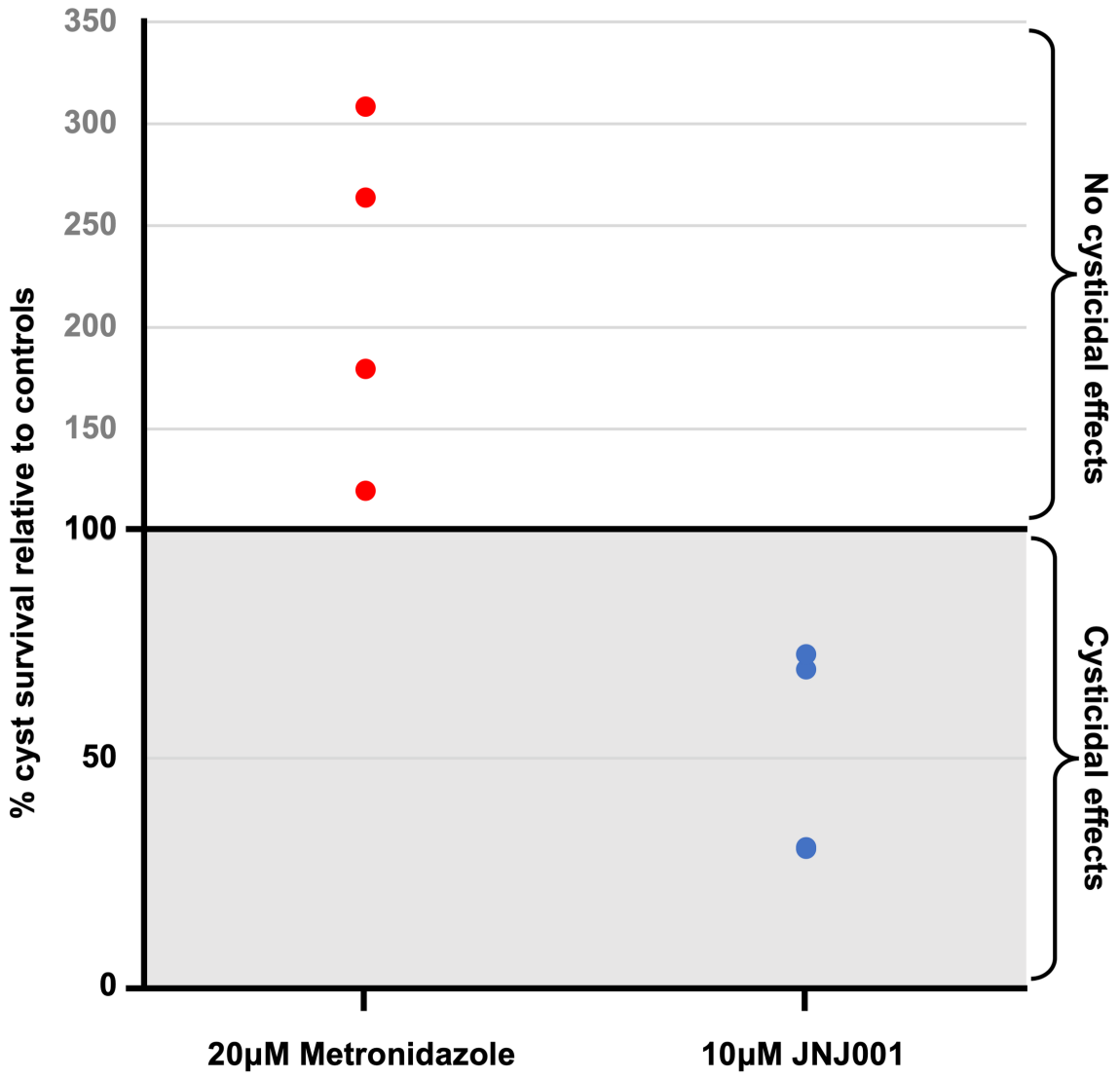

Figure 2.6. Compound JNJ001 inhibits *E. invadens* cysts.
Graph representing survival of luciferase-expressing *E. invadens* cysts treated with 10μM compound JNJ001 (navy blue markers) or 20μM metronidazole (red markers) relative to 0.5% DMSO-treated controls. Markers represent individual luciferase readings. Metronidazole data taken from (Sauvey *et al.*, 2021) [19].

Screen of compounds structurally related to JNJ001 against *E. histolytica* trophozoites

In order to find additional inhibitors of *E. histolytica* based on compound JNJ001, we searched for structurally related compounds in both the hit list from the Jump-stARter library and online chemical vendor catalogs. We began by conducting a structural clustering analysis of the 128 available Jump-stARter library hits from the high-throughput screen. From this clustering analysis we identified 9 structurally similar series expansion compounds (designated as JNJ001-SE01 to JNJ001-SE09) and determined their EC_{50} values using *in vitro* dose-response assays as previously described (Figs 7,8). The resulting values ranged 1.38μM to 6.57μM (Table 2). We next conducted substructure- and similarity-based searches of online chemical vendor catalogs and identified 14 purchasable compounds (designated as CAB01-CAB14) similar to JNJ001. These were then purchased and tested to determine their EC_{50} values (Figs 9,10). The resulting values ranged from 4.53μM to 44.85μM (Table 3). These results together indicate that compound JNJ001 is a member of a structurally-related family of small molecules with anti-amoebic properties.

Table 2.2 EC_{50} values of Jump-stARter library JNJ001 series expansion compounds against *E. histolytica* trophozoites in vitro.

Compound ID:	EC50 (µM)
JNJ001	0.29
JNJ001-SE01	0.54
JNJ001-SE02	1.37
JNJ001-SE03	1.64
JNJ001-SE04	1.72
JNJ001-SE05	3.35
JNJ001-SE06	4.26
JNJ001-SE07	23.60
JNJ001-SE08	26.06
JNJ001-SE09	43.64

EC_{50} values determined from dose-response assay against *E. histolytica* trophozoites in vitro. Color scale indicates compound potency. Green = more potent, red = less potent, grey = no effect.

Table 2.3 EC_{50} values of non-Jump-stARter library JNJ001 series expansion compounds against *E. histolytica* trophozoites in vitro.

Compound ID:	EC_{50} (µM)
CAB07	4.53
CAB10	6.27
CAB09	7.40
CAB05	8.33
CAB11	10.81
CAB12	12.46
CAB02	12.91
CAB13	14.32
CAB14	15.34
CAB08	17.34
CAB04	22.86
CAB06	23.39
CAB01	24.17
CAB03	44.85

EC_{50} values determined from dose-response assay against *E. histolytica* trophozoites in vitro. Color scale indicates compound potency. Green = more potent, red = less potent, grey = no effect.

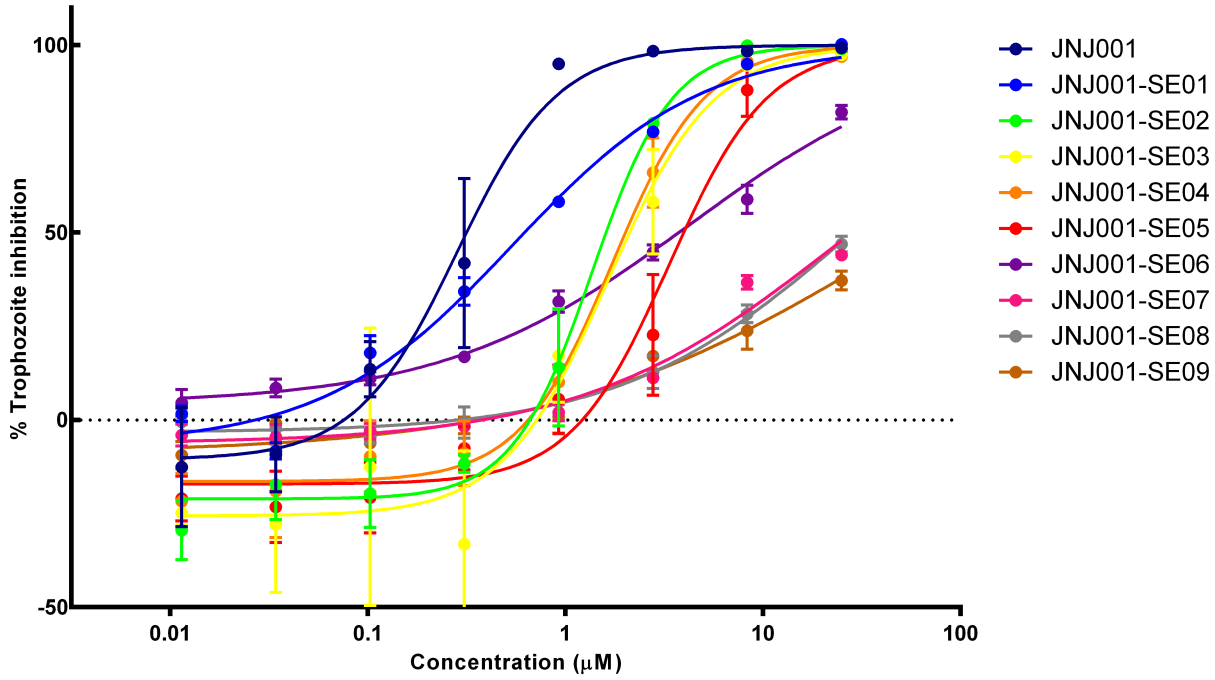

Figure 2.7. Dose-response assay results for Jump-stARter library JNJ001 series expansion compounds.
Dose-response curves show percent inhibition of *E. histolytica* trophozoites compared to compound concentration. Trophozoite cell viability or survival was measured after 48 hours of exposure to test compounds, and percent inhibition for each compound was calculated relative to controls. Compound JNJ001 data (shown as a navy blue line) from Figure 2 is included for comparison. Error bars represent standard deviation.

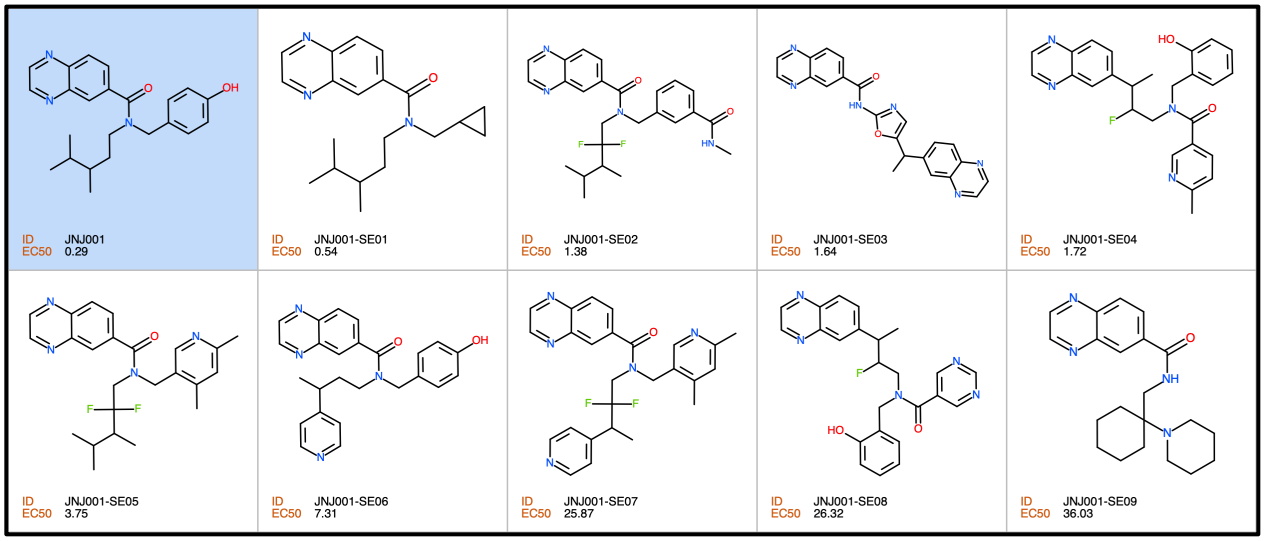

Figure 2.8. Structures of Jump-stARter library JNJ001 series expansion compounds.
Structures, IDs, and measured EC_{50} values of compounds structurally related to JNJ001 (highlighted in blue) found in the Janssen Jump-stARter library.

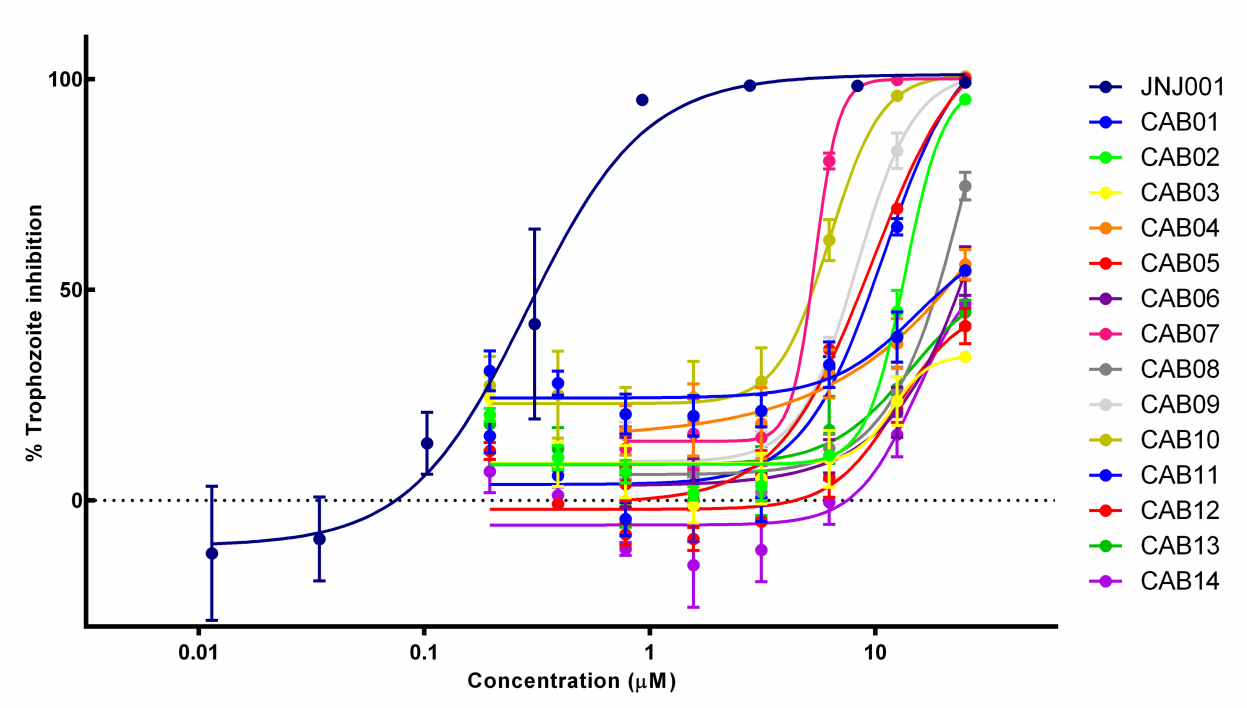

Figure 2.9. Dose-response assay results for non-Jump-stARter library JNJ001 series expansion compounds.
Dose-response curves show percent inhibition of *E. histolytica* trophozoites compared to compound concentration. Trophozoite cell viability or survival was measured after 48 hours of exposure to test compounds, and percent inhibition for each compound was calculated relative to controls. Compound JNJ001 data (shown as a navy blue line) from Figure 2 is included for comparison. Error bars represent standard deviation.

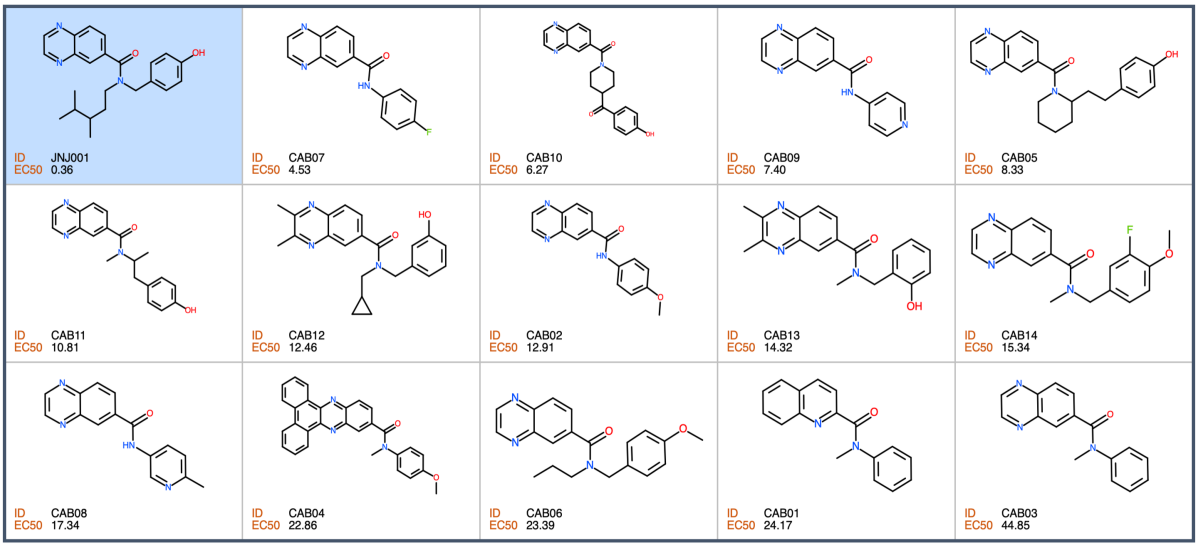

Figure 2.10. Structures of non-Jump-stARter library JNJ001 series expansion compounds. Structures, IDs, and measured EC_{50} values of additional compounds structurally related to JNJ001 (highlighted in blue).

Human cell toxicity assay of series expansion compounds

In order to determine whether, like JNJ001, the series expansion compounds are cytotoxic to human cells, we tested them in a dose-response assay against cultured human HEK293 cells. Of the compounds tested, none produced notable toxicity to the human cells at concentrations up to 25μM (Fig 11). These results indicate that the compounds structurally-related to JNJ001 are not inhibiting *E. histolytica* due to a generalized cytotoxicity.

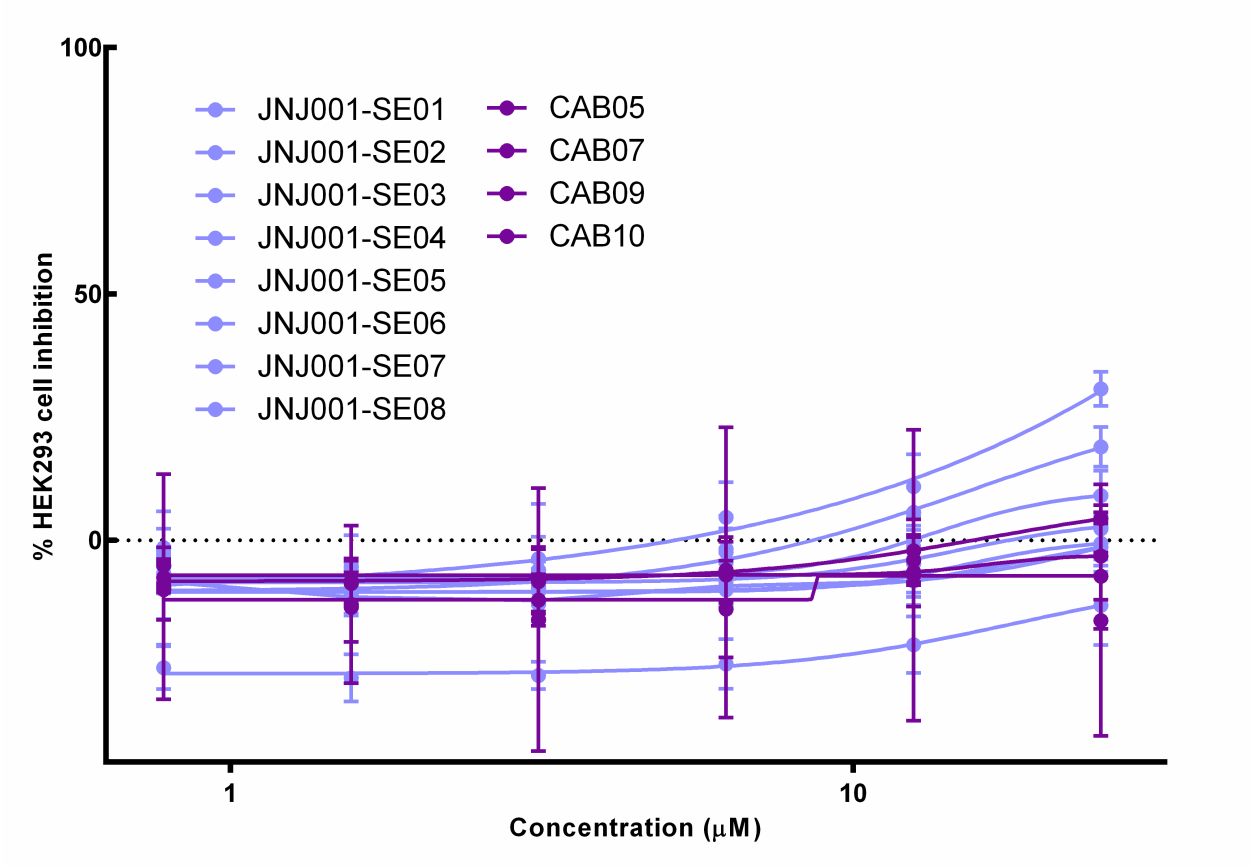

Figure 2.11. Series expansion compounds do not cause cell death in human HEK293 cells. Dose-response curves show percent inhibition of human HEK293 cells compared to compound concentration. Cell viability was measured after 48 hours of exposure to test compounds, and percent inhibition for each compound was calculated relative to positive and negative controls. Jump-stARter library compounds structurally related to JNJ001 are represented with light blue lines. Purchased compounds structurally related to JNJ001 are represented with pink lines. Error bars represent standard deviation.

Discussion

Amoebiasis caused by infection with *E. histolytica* remains a significant public health issue in many places throughout the world, despite the longstanding availability of the drug metronidazole as a treatment [3, 4]. Multiple factors may contribute to this, including infrastructural problems in affected areas such as difficulties with water and food sanitation [4]. However, another important factor may be the shortcomings of metronidazole itself. Strong side effects and metronidazole's inability to kill transmissible cysts complicate the course of treatment and have been suggested to contribute to patient non-compliance and resulting increased disease spread [10, 11]. As such, research into new and better anti-amoebic drugs is ongoing. For much of the history of this research, efforts have focused on inhibiting or disrupting specific cellular processes or targets within the parasite such as redox metabolism or kinase proteins [16]. As an example, authors of this study identified several antineoplastic kinase inhibitor drugs as highly potent inhibitors of *E. histolytica* [19]. More recently however, some groups, including authors of this study, have begun to achieve success with non-targeted screens ranging from low-to-high-throughput [17, 18]. In the current study, we continued and expanded upon this approach by conducting a large high-throughput in vitro screen against *E. histolytica*, resulting in the identification of a promising new family of potent inhibitors of this parasite.

The primary objective of this study was to use a high-throughput screening approach to identify novel small-molecule inhibitors of *E. histolytica* with high potential for further development as treatments for amoebiasis. To achieve this, we began by establishing a set of specific properties which would define an ideal successful candidate compound in our screen. We determined that such a compound would need to meet the following criteria:

Firstly, to possess “drug-like” chemical properties such as appropriate molecular weight, solubility, and lack of known toxic groups. Such properties would be necessary for any further research efforts seeking to develop the compound into a useful drug treatment for amoebiasis.

Secondly, to surpass the current standard of care drug metronidazole in potency. A higher potency could help address several of the drawbacks of metronidazole, such as lowering the dosage required, and potentially reducing adverse effects as a result.

Thirdly, to equal or surpass metronidazole in other measurable attributes such as rapidity of action and non-toxicity to human cells. These are areas that metronidazole performs well in, and any candidate compound would need to at least match it in order to be considered further.
Fourthly, to exhibit inhibitory activity towards *Entamoeba* cysts, unlike metronidazole. A compound capable of any such inhibition would represent a large advantage over metronidazole, as metronidazole’s inability to kill cysts is currently one of its primary drawbacks.

With these four criteria established, we next proceeded to design the overall experimental approach with them in mind. We addressed the first criteria in the core of our design by selecting the Jump-stARter chemical library as the source of compounds for screening. This library was compiled by scientists at Janssen Pharmaceuticals specifically for use in novel drug discovery efforts and has been used in multiple collaborative projects of that nature [22, 23]. The compounds in the library were selected for their “drug-likeness,” having desirable chemical properties for drug development research closely matching those described in our first criteria. They were also selected for structural diversity and clustering into groups of related compounds, thus facilitating expansion of a single hit into a series or family of molecules. The library is also the largest yet screened against *E. histolytica* at over 80,000

compounds, which further increased the probability of identifying a high-potency hit, and thus helped address the second criteria.

However, this large library size also represented the next important challenge in our experimental design. Previous screening efforts against *E. histolytica* have used a maximum number of wells per assay plate of 96 or 384 [17, 18]. In the case of a library of this size, using plates of those well densities would necessitate using hundreds of them, which would result in a lengthy and complicated screening procedure. In order to avoid this and streamline our process we developed and optimized a screening procedure using 1536-well plates, thus drastically reducing the overall number of plates required, and hence the time required for screening them. This technical advance also has the additional benefit of opening up new possibilities of scale for future screening efforts against *E histolytica*.

Once the assay protocol was established, we screened the Jump-stARter library against *E. histolytica* trophozoites *in vitro* using a luciferase-based cell viability assay, which effectively measures the adenosine triphosphate (ATP) contained within surviving cells in each reaction volume, which can in turn be compared with average positive and negative control values to obtain a percent inhibition for each compound screened. We then further tested top-scoring compounds in assays to determine their EC_{50} values, revealing one in particular, compound JNJ001, as highly potent. We calculated the EC_{50} value of this compound as 0.29μM - more than a full order of magnitude greater than the previously established values for metronidazole (2-5 μM), and hence fulfilling our second desired criteria [19]. We confirmed this result with a secondary assay using a direct cell-counting method to show the compound as a true positive hit independent of assay type.

Having identified compound JNJ001 as fulfilling the first two of our desired criteria, we assayed the compound for toxicity to human HEK293 cells in vitro. We found compound JNJ001 (similarly to

metronidazole) to be completely non-toxic at doses up to 25μM, and far exceeding its EC_{50} value. This effectively resulted in a wide therapeutic range spanning from the low tens of nanomolar into the tens of micromolar. We also performed a timecourse assay to compare the compound's rapidity of action with that of metronidazole, and found both it and metronidazole to achieve their final EC_{50} values within 24-36 hours. Together these results confirmed that compound JNJ001 satisfied our third criteria.

Next, we approached our fourth criteria by assaying the ability of compound JNJ001 to inhibit the cysts of *Entamoeba invadens*, a closely-related reptilian parasite. In our experiment, compound JNJ001 was found to moderately inhibit *E. invadens* cysts, whereas metronidazole did not at all. This moderate cysticidal activity represents a significant advantage over metronidazole.

Having successfully identified a compound which fulfilled all of the desired criteria, we next sought to expand upon these results and search for additional related molecules with anti-amoebic activity. We used structural clustering to identify several related molecules within the Jump-stARter library. We also used substructure searching to find and obtain additional structurally-related molecules from commercial sources. We then took these two sets of series expansion compounds and assayed them for both their EC_{50} against *E. histolytica* trophozoites, and their toxicity towards cultured human cells. We found several of the compounds to possess good EC_{50} values, though not as potent as compound JNJ001, and additionally found all of them to possess very low toxicity to human HEK293 cells. These results served as further validation of the anti-amoebic activity of compound JNJ001, confirming that it was not just an isolated phenomenon, but instead can be attributed to a cluster of related molecules with shared activity against this parasite. This discovery also greatly broadened and diversified our set of available

anti-amoebic compounds, providing several additional options for further development, some of which may prove to possess even more desirable chemical properties for that process.

Given the results just discussed, going forward, several areas of further research on JNJ001 and related molecules are now possible. Further studies on the efficacy of these compounds in animal models of *E. histolytica* infection would be valuable, though this will be rendered challenging by the difficulties of establishing and maintaining such models [27, 28]. Similarly, safety and tolerability studies in cultured cells, animal models, and humans would be an essential aspect of developing these into clinical treatments. The possibility also exists and can be explored that these compounds may be effective against other related parasitic species.

One particularly important aspect worth investigation, however, is deconvolution of the specific protein targets of these compounds in *E. histolytica* parasites [29]. For this task, several different approaches are possible, each with their respective strengths and weaknesses [30]. Many of these approaches rely on the use of molecular linkers to immobilize the ligand or attach it to various assay components [30]. However, altering the chemical structure of any ligand of interest by attaching a linker carries the inherent risk of disrupting the binding of that ligand to some or all of its protein targets [30, 31]. Hence success in chemically modifying a compound without disrupting its binding can greatly facilitate the target deconvolution process [30]. A particularly useful family of chemical-linker-based techniques that could be applied here is the various affinity chromatography strategies, wherein the ligand of interest is immobilized on beads, and used to capture and identify target proteins from cell extracts [30, 32]. This type of approach has the advantage of being both relatively uncomplicated and widely used. Its primary downsides other than those inherent to the aforementioned chemical linker stem from a bias

towards identifying more common protein binders of the ligand, though this can be ameliorated with various experimental design strategies [30].

Should chemical-linker-based target deconvolution strategies prove too difficult or disruptive to the functionality of compound JNJ001, alternative approaches are possible. For example, transcriptomic, genomic, and/or proteomic comparisons could be made between parasites which have been selectively pressured to develop resistance to JNJ001 and drug-naïve ones [13, 15, 33]. Such experiments could identify specific genes or gene products which are altered in drug-resistant parasites, possibly including the targets responsible for the compounds anti-amoebic effects. On the other hand, it is quite possible that the parasites in this scenario might acquire resistance solely through downregulation or mutation of transporter or channel proteins in order to block the compound from entering the cell, thus obviating the necessity for any alterations to the actual cellular targets.

Practically speaking, a combination of approaches such as those just discussed would likely be necessary in order to successfully identify candidate targets for JNJ001, with overlapping results serving to reinforce each other. In such a case, further validation could be achieved through the use of RNA-interference-based knockdowns against putative targets, as well as direct binding studies.

Taken together the results described in this study indicate the existence of a promising new family of safe, structurally-related small molecules with strong anti-amoebic properties against both trophozoites and cysts, and good potential for further development as amoebiasis drugs. In conclusion, the discovery of these new anti-amoebic compounds represents an exciting new opportunity in the area of amoebiasis research.

Materials and methods

Compound Library

The chemical compound library screened against *E. histolytica* trophozoites was obtained in collaboration with Janssen Pharmaceuticals. The library, referred to as the "Jump-stARter" library, contains a diverse collection of 80,000 drug-like small molecules intended for maximum potential efficacy in collaboration drug-discovery projects with external research groups [20-23, 25]. The Jump-stARter library was originally selected from millions of proprietary compounds by Janssen Pharmaceuticals medicinal chemists using "drug-likeness," structural diversity, and favorable physical properties as criteria [24, 25]. For this study the library was spotted into black, clear-bottom 1536-well plates (Greiner) at 50nLper well in the Janssen compound logistics facility in Beerse, Belgium, and shipped directly to the University of California - San Diego.

Entamoeba cell culture

E. histolytica strain HM-1:IMSS trophozoites were maintained in 50ml culture flasks (Greiner Bio-One) containing TYI-S-33 media, 10% heat-inactivated adult bovine serum (Sigma), 1% MEM Vitamin Solution (Gibco), supplemented with penicillin (100 U/mL) and streptomycin (100 μg/mL) (Omega Scientific) [17]. *E. invadens* strain IP-1 (a) were cultured in LYI-S-2 (b) at 25°C [34, 35].

High-throughput phenotypic screen

Metronidazole and DMSO controls were added to the pre-spotted 1536-well Jump-stARter library plates using a Multidrop Combi reagent dispenser (Thermo Scientific), resulting in final assay concentrations of 25μM and 0.5% respectively. Cultured *E. histolytica* trophozoites were then seeded into

the same plates at a density of 400 cells per well, also using a Multidrop Combi reagent dispenser, resulting in a final test compound concentration of 25μM. The plates were sealed into GasPak EZ (Becton-Dickinson) bags and incubated at 37°C for 48hr. 2μL of CellTiter-Glo luminescence-based cell viability assay reagent was added using a Multidrop Combi reagent dispenser, and plates were incubated in the dark for 10 minutes. Luminescence was measured using an EnVision plate reader (Perkin Elmer). Percent inhibition values for each well were calculated and plotted using Microsoft Excel. Outlying values and plates resulting from observed technical malfunctions such as clogging or bubbling during liquid handling were excluded from the final analysis.

384-well dose-response cell viability assay

Compounds at 5mM were transferred from a stock plate to black, clear-bottom 384-well plates (brand) and each diluted in DMSO in a 7-point series by a factor of 2. Diluted compounds were then transferred in triplicate into black, clear-bottom 384-well assay plates using an Acoustic Transfer System (EDC Biosystems). Final compound concentrations ranged from 25μM to 0.39μM. Cultured *E. histolytica* trophozoites were added at a density of 1000 cells per well, plates were sealed into GasPak EZ bags and incubated at 37°C for 48hr. CellTiter-Glo reagent was added and luminescence values were measured, and percent inhibition was calculated for each well as described previously.

96-well dose-response EC_{50} determination assay

Cultured *E. histolytica* trophozoites were seeded into white, solid-bottom 96-well plates (Greiner) at a density of 5000 cells per well. Test compounds were diluted in DMSO in 8-point series by a factor of 2 and added to wells in triplicate. 10μM metronidazole and 0.5% DMSO controls were added. Plates were sealed into GasPak EZ bags and incubated at 37°C for 48hr. CellTiter-Glo reagent was added and

luminescence values were measured and percent inhibition was calculated for each well as described previously. EC_{50} values were calculated and dose-response curves were plotted using GraphPad Prism software.

Human cell toxicity assay

HEK293 cells were cultivated in 75cm2 flasks (Corning) containing Dulbecco's modified eagle medium (DMEM) (Gibco) supplemented with 10% fetal bovine serum (FBS) (Gibco) and antibiotic-antimycotic solution (Sigma-Aldritch). Cells were detached by trypsinization, collected, and seeded into (plates) at a density of 5000 cells per well. Test compounds were diluted in DMSO in a 6-point series by a factor of 2 and added to assay wells in quadruplicate alongside 0.5% DMSO and media-only controls. Final assay concentrations ranged from 25μM to 0.78μM. Assay plates were incubated for 48 hours, then CellTiter-glo reagent was added. Assay plates were incubated in the dark for 10 minutes, then luminescence values were read on an EnVision plate reader. Percent inhibition values for each replicate were calculated from luminescence data using Microsoft Excel, and LD50 values were calculated and dose-response curves plotted using GraphPad Prism.

Timecourse assay

Cultured *E. histolytica* trophozoites were plated in 96-well plates at densities of 5000 cells per well. Compounds of interest were serially diluted by a factor of 2 in DMSO to a total of 8 points and added to wells in each replicate plate in triplicate along with 0.5% DMSO and 10μM metronidazole controls. The final in-well concentrations of the compounds of interest ranged from 25μM to 0.195μM. The replicate plates were individually incubated for either 6, 12, 24, 36, or 48 hours, following which

CellTiter-glo reagent was added. Luminescence was measured, EC_{50} values were determined, and dose-response curves were plotted as described previously.

Cyst viability assay

Mature cyst viability assay was performed as described previously, using a transgenic *E. invadens* line stably expressing luciferase (CK-luc) [16, 22]. Parasites were induced to encyst by incubation in encystation media (47% LG) [23]. After 72 h, parasites were washed once in distilled water and incubated at 25°C for 4–5 h in water to lyse trophozoites. Purified cysts were pelleted, counted to ensure equal cyst numbers, and resuspended in encystation media at a concentration of 1-5x105 cells per ml. One ml suspension per replicate was transferred to glass tubes containing encystation media and drug or DMSO, then incubated at 25°C for 72 h. On the day of the assay, cysts were pelleted and treated once more with distilled water for 5 h to lyse any trophozoites that had emerged during treatment. Purified cysts were then resuspended in 75 µl Cell Lysis buffer (Promega) and sonicated for 2x10 seconds to break the cyst wall. Luciferase assay was performed using the Promega luciferase assay kit according to the manufacturer's instructions. Assays were performed on equal volume of lysate (35 µl) and not normalized to protein content. Effect of the drug was calculated by comparison to DMSO control, after subtraction of background signal. Significance of drug effects was calculated using a one-tailed T-test.

Funding acknowledgments

This work was supported in part by the Janssen Pharmaceuticals / UCSD Biomedical Sciences Program Graduate Student Collaboration 2019. R.A. received funding from the United States National Institute of Health National Institute of General Medical Sciences grant R35GM131881. G.E. received funding from the National Institute of Allergy and Infectious Diseases Grant R21AI146651.

Author Contributions

Conceptualization, C.S., J.B., R.A.; Methodology, C.S., G.E., J.B.; Formal Analysis, C.S.; Data Curation, C.S.; Writing – Original Draft, C.S.; Visualization, C.S.; Supervision, R.A., P.J., J.B.; Funding Acquisition, R.A., P.J.; Writing – review & editing, C.S., G.E., J.B., and R.A.

Competing Interests

The authors declare that they have no conflicts of interest.

Chapter 2, in part, has been submitted for publication of the material as it may appear in PLOS Neglected Tropical Diseases, 2021, Conall Sauvey, Gretchen Ehrenkaufer, Jonathan Blevitt, Paul Jackson, Ruben Abagyan. The dissertation author was the primary investigator and author of this paper.

References:

1. Pritt BS, Clark CG. Amebiasis. Mayo Clin Proc. 2008;83(10):1154-9; quiz 9-60.

2. Shirley DT, Farr L, Watanabe K, Moonah S. A Review of the Global Burden, New Diagnostics, and Current Therapeutics for Amebiasis. Open forum infectious diseases. 2018;5(7):ofy161.

3. Carrero JC, Reyes-Lopez M, Serrano-Luna J, Shibayama M, Unzueta J, Leon-Sicairos N, de la Garza M. Intestinal amoebiasis: 160 years of its first detection and still remains as a health problem in developing countries. Int J Med Microbiol. 2020;310(1):151358.

4. Shirley DT, Watanabe K, Moonah S. Significance of amebiasis: 10 reasons why neglecting amebiasis might come back to bite us in the gut. PLoS Negl Trop Dis. 2019;13(11):e0007744.

5. Faria CP, Zanini GM, Dias GS, da Silva S, de Freitas MB, Almendra R, Santana P, Sousa MD. Geospatial distribution of intestinal parasitic infections in Rio de Janeiro (Brazil) and its association with social determinants. PLoS Negl Trop Dis. 2017;11(3):e0005445.

6. Sahimin N, Lim YA, Ariffin F, Behnke JM, Lewis JW, Mohd Zain SN. Migrant Workers in Malaysia: Current Implications of Sociodemographic and Environmental Characteristics in the Transmission of Intestinal Parasitic Infections. PLoS Negl Trop Dis. 2016;10(11):e0005110.

7. Ralston KS, Petri WA, Jr. Tissue destruction and invasion by Entamoeba histolytica. Trends in parasitology. 2011;27(6):254-63.

8. Petri WA, Haque R. Entamoeba histolytica brain abscess. Handbook of clinical neurology. 2013;114:147-52.

9. Marie C, Petri WA, Jr. Amoebic dysentery. BMJ clinical evidence. 2013;2013.

10. Garduno-Espinosa J, Martinez-Garcia MC, Fajardo-Gutierrez A, Ortega-Alvarez M, Alvarez-Espinosa A, Vega-Perez V, Munoz-Hernandez O. Frequency and risk factors associated with metronidazole therapeutic noncompliance. Revista de investigacion clinica; organo del Hospital de Enfermedades de la Nutricion. 1992;44(2):235-40.

11. Dusengeyezu E, Kadima J. How do Metronidazole Drawbacks Impact Patient Compliance and Therapeutic Outcomes in Treating Amoebiasis in Rwanda. International Journal of TROPICAL DISEASE & Health. 2016;17(3):1-7.

12. Kikuchi T, Koga M, Shimizu S, Miura T, Maruyama H, Kimura M. Efficacy and safety of paromomycin for treating amebiasis in Japan. Parasitology international. 2013;62(6):497-501.

13. Wassmann C, Hellberg A, Tannich E, Bruchhaus I. Metronidazole resistance in the protozoan parasite Entamoeba histolytica is associated with increased expression of iron-containing superoxide dismutase and peroxiredoxin and decreased expression of ferredoxin 1 and flavin reductase. The Journal of biological chemistry. 1999;274(37):26051-6.

14. Edwards DI. Nitroimidazole drugs--action and resistance mechanisms. I. Mechanisms of action. The Journal of antimicrobial chemotherapy. 1993;31(1):9-20.

15. Penuliar GM, Nakada-Tsukui K, Nozaki T. Phenotypic and transcriptional profiling in Entamoeba histolytica reveal costs to fitness and adaptive responses associated with metronidazole resistance. Front Microbiol. 2015;6:354.

16. Shrivastav MT, Malik Z, Somlata. Revisiting Drug Development Against the Neglected Tropical Disease, Amebiasis. Front Cell Infect Microbiol. 2020;10:628257.

17. Debnath A, Parsonage D, Andrade RM, He C, Cobo ER, Hirata K, Chen S, Garcia-Rivera G, Orozco E, Martinez MB, Gunatilleke SS, Barrios AM, Arkin MR, Poole LB, McKerrow JH, Reed SL. A high-throughput drug screen for Entamoeba histolytica identifies a new lead and target. Nat Med. 2012;18(6):956-60.

18. Ehrenkaufer GM, Suresh S, Solow-Cordero D, Singh U. High-Throughput Screening of Entamoeba Identifies Compounds Which Target Both Life Cycle Stages and Which Are Effective Against Metronidazole Resistant Parasites. Front Cell Infect Microbiol. 2018;8:276.

19. Sauvey C, Ehrenkaufer G, Shi D, Debnath A, Abagyan R. Antineoplastic kinase inhibitors: A new class of potent anti-amoebic compounds. PLoS Negl Trop Dis. 2021;15(2):e0008425.

20. Inc. JP. Global Public Health [Available from: https://jnjinnovation.com/partnering/global-public-health.

21. Janssen Pharmaceuticals I. Accelerating Innovation Worldwide. Janssen Pharmaceuticals.

22. Bailey BL, Nguyen W, Ngo A, Goodman CD, Gancheva MR, Favuzza P, Sanz LM, Gamo FJ, Lowes KN, McFadden GI, Wilson DW, Laleu B, Brand S, Jackson PF, Cowman AF, Sleebs BE. Optimisation of 2-(N-phenyl carboxamide) triazolopyrimidine antimalarials with moderate to slow acting erythrocytic stage activity. Bioorg Chem. 2021:105244.

23. Nizami S, Millar V, Arunasalam K, Zarganes-Tzitzikas T, Brough D, Tresadern G, Brennan PE, Davis JB, Ebner D, Di Daniel E. A phenotypic high-content, high-throughput screen identifies inhibitors of NLRP3 inflammasome activation. Sci Rep. 2021;11(1):15319.

24. Hann MM, Oprea TI. Pursuing the leadlikeness concept in pharmaceutical research. Curr Opin Chem Biol. 2004;8(3):255-63.

25. Re:Search W. WIPO Re:Search Partnership Stories 2016-2019 [Available from: https://bvgh.org/wp-content/uploads/2019/11/WIPO-ReSearch-Partnership-Stories-2016-2019.pdf.

26. Sanchez L, Enea V, Eichinger D. Identification of a developmentally regulated transcript expressed during encystation of Entamoeba invadens. Mol Biochem Parasitol. 1994;67(1):125-35.

27. Tsutsumi V, Shibayama M. Experimental amebiasis: a selected review of some in vivo models. Archives of medical research. 2006;37(2):210-20.

28. Hamano S, Becker S, Asgharpour A, Ocasio YP, Stroup SE, McDuffie M, Houpt E. Gender and genetic control of resistance to intestinal amebiasis in inbred mice. Genes Immun. 2008;9(5):452-61.

29. Lee JA, Berg EL. Neoclassic drug discovery: the case for lead generation using phenotypic and functional approaches. J Biomol Screen. 2013;18(10):1143-55.

30. Terstappen GC, Schlüpen C, Raggiaschi R, Gaviraghi G. Target deconvolution strategies in drug discovery. Nat Rev Drug Discov. 2007;6(11):891-903.

31. Saxena C. Identification of protein binding partners of small molecules using label-free methods. Expert Opin Drug Discov. 2016;11(10):1017-25.

32. Saxena C, Higgs RE, Zhen E, Hale JE. Small-molecule affinity chromatography coupled mass spectrometry for drug target deconvolution. Expert Opin Drug Discov. 2009;4(7):701-14.

33. Uzlikova M, Nohynkova E. The effect of metronidazole on the cell cycle and DNA in metronidazole-susceptible and -resistant Giardia cell lines. Mol Biochem Parasitol. 2014;198(2):75-81.

34. Clark CG, Diamond LS. Methods for cultivation of luminal parasitic protists of clinical importance. Clinical microbiology reviews. 2002;15(3):329-41.

35. Meerovitch E. A NEW HOST OF ENTAMOEBA INVADENS RODHAIN, 1934. Canadian Journal of Zoology. 1958;36(3):423-7.

Supporting information

Supplementary dataset 2.1 Figure 1 data. (XLSX)

Supplementary dataset 2.2 384-well dose-response screen data. (XLSX)

Supplementary dataset 2.3 Figure 2 data. (XLSX)

Supplementary dataset 2.4 Figure 3 data. (XLSX)

Supplementary dataset 2.5 Figure 4 data. (XLSX)

Supplementary dataset 2.6 Figure 5 data. (XLSX)

Supplementary dataset 2.7 Figure 6 data. (XLSX)

Supplementary dataset 2.8 Figure 7 data. (XLSX)

Supplementary dataset 2.9 Figure 9 data. (XLSX)

Supplementary dataset 2.10 Figure 11 data. (XLSX)